

INVESTIGATION OF GPCR ACTIVATION BY HEALTHY AND INSULIN-RESISTANT
ADIPOCYTES

BY

MAGGIE M. PICKARD

A thesis submitted to the
Department of Chemistry and Biochemistry
Mount Allison University
in partial fulfillment of the requirements for the
Bachelor of Science degree with Honours
April 23rd, 2021

Abstract

In obesity, chronic caloric excess results in maladaptive secretion of adipokine hormones from over-expanded adipose tissues. These secretions are critical in the development of insulin-resistance and type II diabetes. Many adipokines are endogenous ligands to G protein-coupled receptors (GPCR). Thus, it is possible that these disease-modulating hormones are connected to GPCRs with currently unidentified endogenous ligands, orphan GPCRs. The aim of this study was to identify if orphan GPCRs are adipokine sensing receptors and can detect the difference between healthy and insulin-resistant adipocytes. This was achieved through the screening of healthy and insulin-resistant adipocyte-conditioned media against 71 orphan GPCRs. Receptor activation was quantified using the PRESTO-Tango β -arrestin recruitment assay. Adipocyte-conditioned media significantly altered the activation of 19 receptor candidates. Further, insulin-resistant adipocyte conditioned media significantly altered the activation of GPR17, GPR45 and GPR54 relative to healthy adipocyte-conditioned media. This led to a recommendation of 12 receptor candidates for further investigation. The activation of these twelve receptors was summarized into three categories: 1) receptors significantly activated by both adipocyte-conditioned media 2) receptors with significantly decreased activation by both adipocyte-conditioned media and 3) receptors that were differentially activated between the two adipocyte-conditioned media. These findings demonstrate the diverse connections between adipocytes and the receptor candidates. Further investigation into the 12 receptor candidates will lead to greater knowledge about the function of these elusive receptors. This will aid in identifying endogenous ligands for these receptor candidates, and in the application of these findings to the development of therapeutic treatments for type II diabetes.

Acknowledgements

I would like to first thank my supervisor and the most incredible mentor, Dr. Jillian Rourke for her endless support and guidance throughout the entirety of this project. Thank you for introducing me to the world of research, for answering my endless questions, supporting me through this wild and stressful year, and for teaching me how fun and exciting research can be. I would also like to thank my second reader, Dr. Amanda Cockshutt, for her helpful guidance. Another special thanks to Dr. Tyson MacCormack, for the use of his lab space and equipment for luciferase assays, and for being an incredible professor these last few years. Thank you to the entire team in the Sinal Lab at Dalhousie University, especially to Nichole McMullen for preparing the adipocyte treatments for use in this study. Thank you to Maddy Russell, for performing the cell culture leg work on the high throughput screen, and for the endless guidance, tips, and training throughout this summer. You were endlessly helpful and made the summer in the lab so fun. To the rest of my lab mates – Madeline, thank you for all your help and guidance this year, Alexie, thank you for being a great member of the lab team and Hannah; thank you for always being there to talk things through and calm me down, and for company for all the long hours in the flex lab! I could not have done this without you – this thesis, or really any part of the last few years of this degree. Special thanks to Mount Allison University, NSERC, NBIF, and NBHRF for funding this research project. Thank you to my parents, without whom I would not be at Mount Allison University and would have never had the chance to complete this honours project. With that, thank you both so much for all the support and for always looking to hear about this project, even when you swore the only word in it you understood was diabetes! Finally, thanks to all my friends and family who listened to me, made me laugh, and kept me sane through it all this year. I am incredibly grateful to have the best support system to have helped me get where I am today.

Table of Contents

Abstract	2
Acknowledgements	3
List of Figures and Tables.....	6
List of Figures and Tables in Appendix.....	8
Glossary of abbreviations and symbols	9
1. Introduction	11
1.1 Obesity: Causes, prevalence, and disease markers	11
1.2 Obesity, insulin resistance & type II diabetes	11
1.3 Modelling insulin resistance to discover potential treatments	14
1.4 G Protein Coupled Receptors	16
1.5 GPCR's as drug targets	17
1.6 Measuring GPCR activation: The Tango assay.....	18
1.7 High throughput screening: PRESTO-Tango luciferase assay.....	20
1.8 Adipokines as GPCR ligands	21
1.9 Summary and Scope of Study	21
2. Materials and Methods.....	22
2.1 Cell culture	22
2.2 DNA purification	22
2.3 Treatment preparation: Adipocyte-conditioned media	22
2.4 PRESTO TANGO assay	23
2.4.1 Plating.....	23
2.4.2 Transfection	23
2.4.3 Treatment and lysis	23
2.4.4 Luciferase and β -gal assays	23
2.5 Statistical analyses and data transformation.....	24
3. Results.....	25
3.1 LPAR1 acts as a control for assay quality.....	25
3.2 Adipocyte-conditioned media activates known adipokine receptors.....	26
3.3 Orphan receptors differ in basal activation levels	28
3.4 Orphan receptors are differentially activated in response to adipocyte-conditioned media.....	29

3.5 Adipocyte-conditioned media significantly alters activation of 19 receptor candidates	30
3.6 Insulin-resistant adipocyte-conditioned media significantly alters receptor activation.	31
3.7 TNF- α modulates activation of three receptor candidates	32
3.8 Summary and interpretation of results	34
4. Discussion	35
4.1 Adipocyte-conditioned media contains endogenous ligands LPA and ACKR3	36
4.2 Categorizing receptor activation.....	37
4.3 Receptors that were activated by both treatments	38
4.3.1 GPR151	38
4.3.2 GPR61	39
4.3.3 GPR78	40
4.3.4 GPR87	40
4.3.5 TAAR9	41
4.4 Receptors that had decreased activation in response to both treatments	42
4.5 Receptors differentially activated between adipocyte-conditioned media treatments...	43
4.5.1 GPR17	43
4.5.2 GPR45	45
4.5.3 GPR54	45
4.5.4 GPR142	46
4.5.5 GPR153	47
4.5.6 MAS1	48
4.6 Conclusions and further directions	49
5. References	50
6. Appendix	57

List of Figures and Tables

Figure 1: Insulin signaling pathway under normal and insulin-resistant conditions. A) Schematic demonstrating normal insulin signaling activated by the presence of insulin, leading to activation of the PI3K/AKT signaling pathway and glucose release stimulated by glucose GLUT4 translocation to the membrane. B) Release of TNF- α in response inflammation leads to activation of JNK and the subsequent phosphorylation of IRS-1 and the insulin signaling pathway, interrupting GLUT4 translocation and leading to insulin resistance in the cell.	14
Figure 2: Signal Transduction in the Tango Assay. A) Schematic of typical GPCR activation triggered by ligand binding, leading to a signalling cascade B) GPCR activation in the Tango assay: β -arrestin recruitment triggered by ligand binding receptor activation, leading to tTA translocation and reporter gene activation.	19
Figure 3: PRESTO-Tango Plasmid. Design of PRESTO-Tango modified plasmid receptor gene. Image adapted from Kroeze et al. (2015).	21
Figure 4: Schematic outlining the experimental timeline of the PRESTO-Tango assay in the HTS experiment. HTLA cells were plated at 10,000 cells/well prior to a 24-hour incubation period, after which they were transfected with pBSK (empty vector), PCMV- β galactosidase (β -gal), and the PRESTO-Tango GPCR of interest using polyethyleneimine (PEI). 18 hours later, cells were treated with Opti-MEM, MEM- α or adipocyte conditioned media and incubated for another 24 hours prior to lysis and storage at -80°C . Receptor activity was then quantified via luciferase and β gal assays.	24
Figure 5: Significant and dose dependent activation of LPAR1-transfected cells upon treatment with endogenous ligand LPA allows LPAR1 to act as a control for assay quality. Activation of LPAR1 was quantified following a β -arrestin recruitment assay in which HTLA cells were transiently transfected with the receptor. A) The Relative Luminescence units (RLU) adjusted by β -galactosidase expression (A420; RLU/A420) of LPAR1 receptor-transfected cells versus log ₁₀ treatment concentration of LPA. B) The RLU/A420 Fold-Change data for A. C) The RLU/A420 of LPAR1 transfected cells after treatment with Opti-MEM and LPA containing 10% Fetal Bovine Serum (FBS) in Opti-Mem. D) The RLU/A420 Fold-Change data for C. All data is presented as mean with SEM across three biological replicates. Non-linear regression fit models were applied in Prism to A and B, from which an experimental EC ₅₀ of 2.28E-07 M was calculated. ****p<0.0001. ...	26
Figure 6: 3T3-L1 adipocyte-conditioned media significantly activates bioactive lipid receptor and atypical chemokine-receptor 3. Receptor activation was quantified following a β -arrestin recruitment assay in which HTLA cells were transiently transfected with GPCRs as indicated. A) The relative luminescence units (RLU) adjusted by β -galactosidase expression (A420; RLU/A420) of HTLA cells transfected with LPAR1 and ACKR3 after treatment with Opti-Mem (black), unconditioned adipocyte differentiation medium (vehicle; light grey), healthy adipocyte-conditioned media (dark grey), and insulin-resistant adipocyte-conditioned media (white). B) The RLU/A420 Fold-Change data from A C) The RLU/A420 of HTLA cells transfected with LPAR1 after treatment with Opti-MEM or 2.5 nM TNF- α in Opti-MEM. Bar plots are mean with SEM. D) Fold-Change data from C. E) The RLU/A420 of HTLA cells transfected with CMKLR1, CXCR2 or FFAR1 after treatment	

with Opti-Mem (black), unconditioned adipocyte differentiation medium (vehicle; light grey), healthy adipocyte-conditioned media (dark grey), and insulin-resistant adipocyte-conditioned media (white). F) The RLU/A420 Fold-Change data from C. plots are mean with SEM. **** $p < 0.0001$, *** $p < 0.0005$28

Figure 7: Vehicle treatment significantly decreases RLU/A420 for R37 and orphan GPCRs differ in baseline activation levels. RLU/A420 of cells transfected with 72 orphan receptors after treatment with Opti-MEM (black) or unconditioned adipocyte differentiation medium (vehicle;grey). Data presented as mean with SEM. * $p < 0.0001$29

Figure 8: Heat Map of Fold-Change in HTLA cells transfected with 71 orphan receptors following treatment with Healthy or Insulin-Resistant Adipocyte-conditioned media. RLU/A420 fold-change ranging from 0.1-0.499 (dark blue) to 4-7 (dark red) of orphan receptor- transfected cells treated with healthy adipocyte-conditioned media (top) and insulin-resistant adipocyte-conditioned media (bottom). RLU/A420 fold-change is measured relative to RLU/A420 with Opti-MEM treatment. Baseline values (1.76-3.99; white) are representative of the average range of RLU/A420 fold-change of receptors after Opti-MEM treatment.30

Figure 9: 19 Receptor candidates are significantly and differentially activated in response to adipocyte-conditioned media as compared to controls. Receptor activation was quantified following a β -arrestin recruitment assay in which HTLA cells were transiently transfected with GPCR TANGO plasmids. A) RLU/A420 of GPCR transfected cells whose activity was significantly altered in response to treatment with Healthy Adipocyte Conditioned Media (light grey) and/or Insulin-Resistant Adipocyte Conditioned Media (Dark grey) as compared to baseline activation after treatment with Opti-MEM (Black). B) The Fold-Change data from A. Data is presented as mean and SEM, * $p < 0.05$, ** $p < 0.005$, *** $p < 0.0005$, **** $p < 0.0001$31

Figure 10: Three receptor candidates are differentially activated in response to treatment with healthy and insulin resistant adipocyte-conditioned media. Receptor activation was quantified following a β -arrestin recruitment assay in which HTLA cells were transiently transfected with GPCR TANGO plasmids. A) RLU/A420 of GPCR TANGO receptors whose activity was significantly altered after treatment of HTLA cells with healthy-adipocyte conditioned media (grey) as compared to treatment with insulin-resistant adipocyte-conditioned media (black). B) RLU/A420 Fold-Change data for A. Fold-Change was measured relative to RLU/A420 of receptor-transfected cells treated with Opti-MEM (Figure 5). Data is presented as mean and SEM, * $p < 0.05$, ** $p < 0.005$, *** $p < 0.0005$32

Figure 11: Treatment of receptor transfected HTLA cells with 2.5 nM TNF- α significantly alters the activity of GPR153, GPR45 and GPR17. Receptor activation was quantified following a β -arrestin recruitment assay in which HTLA cells were transiently transfected with GPCR TANGO plasmids. A) RLU/A420 of transfected GPCR TANGO receptors after treatment of HTLA cells with 2.5 nM TNF- α (grey) as compared to treatment with Opti-MEM control (Black) B) RLU/A420 Fold-Change data for A, measured relative to RLU/A420 of receptor-transfected cells treated with Opti-MEM. Data is presented as mean and SEM, * $p < 0.05$, ** $p < 0.005$34

Table 1: Interpretation of HTS results: Receptor candidates recommended for further investigation. Fold-Change values relative to Opti-MEM and significance levels (p-values) relative to Opti-MEM of 12 receptor candidates recommended for validation studies after treatment with healthy and insulin-resistant adipocyte-conditioned media in the HTS. p-values between adipocyte-conditioned media treatments for the 12 receptors also presented, as well as p-values from treatment with TNF- α relative to Opti-MEM, if follow up study already completed. *p<0.05 35

List of Figures and Tables in Appendix

Appendix 1: TNF-α induces in vivo insulin resistance. Western blot analysis of phosphor-Akt protein expression from untreated (3T3-L1) and TNF- α treated (3T3-L1 + TNF α) 3T3-L1 adipocytes. Bottom panel shows quantification of protein level normalized to total Akt loading control.....	57
Appendix 2: High Throughput Screen Results. The Fold-Change values relative to Opti-MEM of receptors from the HTS after treatment with healthy and insulin-resistant adipocyte-conditioned media. Data is presented as mean \pm SEM.....	58
Appendix 3: Dose-Dependent Activation of GPR153 in response to treatment with TNFα. Activation of GPR153 was quantified following a β -arrestin recruitment assay in which HTLA cells were transiently transfected with the receptor. A) The Relative Luminescence units (RLU) adjusted by β -galactosidase expression (A420; RLU/A420) of GPR153-transfected cells versus log ₁₀ treatment concentration of TNF- α . B) The RLU/A420 Fold-Change data for A. Non-linear regression fit models were applied in Prism to A and B, from which an experimental EC ₅₀ of 2.56E-09 M was calculated.....	60

Glossary of abbreviations and symbols

7TM – Seven Trans-Membrane
ACKR3 – Atypical Chemokine Receptor 3
AKT – Protein Kinase B
Ang - Angiotensin
ANOVA – Analysis of Variance
BMI – Body Mass Index
cAMP – Cyclic Adenosine Monophosphate
CMKLR1 – Chemerin Receptor 1
CXCL11 - C-X-C Motif Chemokine Ligand 11
CXCL12 - C-X-C Motif Chemokine Ligand 12
CXCR2 - C-X-C Motif Chemokine Receptor 2
cysLT – Cysteinyl Leukotriene
DMEM – Dulbecco's Modified Eagle Medium
DMSO – DiMethyl Sulfoxide
EC50 - Half maximal effective concentration
EDTA - Ethylenediaminetetraacetic Acid
FBS – Fetal Bovine Serum
FDA - Food and Drug Administration
FFA – Free Fatty Acid
FFAR1 – Free Fatty Acid Receptor 1
GEF – Guanine Nucleotide Exchange Factor
GLUT4 – Glucose Transporter 4
GPCR – G-Protein Coupled Receptor
GRK – G-protein coupled receptor kinases
HA – Hemagglutinin
HEK-293 – Human embryonic kidney 293 cells
HTLA cells- Modified (HEK293) cell line stably expressing tTA-dependent luciferase reporter gene and a β -arrestin2-TEV fusion gene

HTS – High Throughput Screen

IRS-1 – Insulin receptor substrate 1

JNK – Jun N Terminal Kinase

Kp - Kisspeptin

LB – Lysogeny Broth

LPA - Lysophosphatidic Acid

LPAR1 – Lysophosphatidic Acid Receptor

NPY - neuropeptide Y

ONPG – Ortho-nitrophenyl- β -galactosidase

PEI – Polyethyleneimine

PI3K - Phosphatidylinositol 3-kinase

PRESTO-Tango- Parallel Receptor-ome Expression and Screening *via* Transcriptional Output-Tango

RGS - Regulators of G protein Signaling

RLU – Relative Luminescence Units

SDF – Stromal Derived Factor

TAAR – Trace amine associated receptor

TEV – Tobacco Etch Virus (TEV)

TNF- α – Tumor Necrosis Factor- α

tTA – Tetracycline transactivator

VEH – Vehicle

β -gal – β -galactosidase

1. Introduction

1.1 Obesity: Causes, prevalence, and disease markers

Obesity is a chronic, progressive disease, making the obesity epidemic a strong cause of concern for health professionals (Hurt *et al.*, 2010). The many associated risks and causal risk factors of obesity are often discussed and warned about in news and media (Blüher, 2019). The disease is positively correlated with higher body mass and diagnoses are made at body mass index (BMI) levels greater than 40 kg/m² (Hurt *et al.*, 2010; Sikaris, 2004). The prevalence of obesity has been increasing since the 1960's, and as of 2016 over 650 million adults and 378 million children worldwide are affected by obesity (Blüher, 2019). Many believe that imbalances caused by excessive caloric intake and lower caloric expenditure are the leading causes of obesity (Blüher, 2019). However, obesity is positively correlated with metabolic dysfunction and dysregulation of hormones responsible for the maintenance of energy homeostasis, making the disease more than just a matter of overconsumption and lack of exercise (Hurt *et al.*, 2010) For example, leptin, the hunger inhibition hormone, can be inhibited in the brain of people with obesity, diminishing the ability of the brain to sense satiety, resulting in overconsumption (Hurt *et al.*, 2010).

Obesity is a risk factor for several different diseases. It is positively correlated to hypertension, and thus the increased risk of heart disease, heart attacks and strokes. Obesity is also associated with an increase in the risk for the development of several types of cancer, musculoskeletal disorders, and Alzheimer's disease (Hurt *et al.*, 2010). Finally, obesity disrupts the metabolic function of insulin and is associated with type II diabetes mellitus and fatty liver disease, due to the accumulation of fat tissue (Hurt *et al.*, 2010).

1.2 Obesity, insulin resistance & type II diabetes

Obesity is one of the leading risk factors for type II diabetes mellitus, with over 90% of people with type II diabetes having a BMI classified as overweight or obese (Sikaris, 2004). Obesity mediates insulin resistance, which results overall in the impaired transport of glucose. Type II diabetes develops when the degree of insulin resistance surpasses the ability of beta cells to produce insulin (Sikaris, 2004). Insulin controls glucose homeostasis and its uptake into target cells in the muscle, liver, and adipose tissue. Glucose transporter 4

(GLUT4) mediates insulin stimulated-glucose uptake into target cells (Ijuin and Takenawa, 2012). The presence of insulin activates the insulin receptor substrate (IRS) and its downstream pathways, such as the phosphatidylinositol 3-kinase (PI3K)/Protein Kinase B (AKT) pathway (Fig. 1). This leads to the translocation of GLUT4 to the membrane, allowing glucose uptake into target cells (Fig. 1A; Ijuin and Takenawa, 2012). Disruptions to this pathway during chronic energy excess and obesity, such as the phosphorylation of IRS-1 serine residues by several different protein kinases, inhibit insulin signaling to GLUT4 (Fig. 1B). This renders the body unresponsive or resistant to insulin (Ijuin and Takenawa, 2012). Under these insulin resistant conditions, glucose transport is impaired, and target cells are unable to take up glucose, resulting in impaired glucose homeostasis (Ijuin and Takenawa, 2012). Insulin resistant models in skeletal muscle have shown decreased levels of GLUT-4- trafficking mediated glucose production and lower glycogen synthesis, resulting in overall decreased glucose uptake in response to insulin resistance (Mueckler, 2001).

Aside from mediating glucose transport, insulin also regulates blood glucose levels by limiting gluconeogenesis. Therefore, the development of insulin-resistance will increase gluconeogenesis. Another role of insulin is to promote the storage of fatty acids in adipose and tissues, meaning that resistance to insulin leads to elevated levels of circulating free fatty acids (FFA) (Sikaris, 2004). Many studies demonstrated that these elevated levels of FFA are also an important contributor to the development of insulin resistance in those with obesity, forming a positive feedback loop (Sikaris, 2004). FFA accumulation contributes to insulin resistance in skeletal muscle by inhibiting insulin mediated glucose transport and to hepatic (liver-related) insulin resistance by blocking insulin's inhibition of glycogenolysis (Zhao *et al.*, 2010). Hepatic insulin resistance also stimulates fatty acid synthesis, creating a positive feedback loop for further FFA accumulation. (Boden, 2003; Hardy *et al.*, 2012). This demonstrates that any suppression of insulin's activity by free fatty acids occurs downstream of insulin production, but that there is a correlation between the accumulation of fatty acids found in obesity and resulting insulin resistance in the liver and skeletal muscle (Boden, 2003). Therefore, FFA accumulation is an important contributor to the development of insulin resistance.

Inflammation is also hypothesized to explain the correlation between obesity, insulin resistance and the onset of type II diabetes. Adipocytes are the most abundant cells of adipose

tissue, and act as storage depots for lipids (Kahn and Flier, 2000). Adipocytes are also endocrine cells, producing adipokine hormones, peptide hormones and cytokines. Adipokines are modulators of hemostasis, blood pressure, atherosclerosis, as well as lipid and glucose metabolism (Fuster *et al.*, 2016; Rabe *et al.*, 2008). Adipokines are categorized as pro-inflammatory or anti-inflammatory adipokines (Rabe *et al.*, 2008). Under obese conditions, excessive caloric intake and fat accumulation leads to adipose tissue expansion. This results in the maladaptive adipokine secretion while insulin resistance also decreases lipolysis in adipose tissue, exacerbating lipid accumulation in adipose tissue (Fuster *et al.*, 2016). Obese conditions result in the upregulation of pro-inflammatory adipokines, that are positively correlated with the development of insulin resistance, forming the inflammatory hypothesis that connects insulin resistance to obesity (Rabe *et al.*, 2008).

Adipokine-mediated insulin resistance in obesity is highly correlated to the inflammatory immune response in altered adipose tissue. This imbalance between pro- and anti-inflammatory adipokines leads to the activation of inflammatory macrophages that secrete inflammatory cytokines such as tumor necrosis factor α (TNF- α) and Interleukin-6 (Kwon and Pessin, 2013). These inflammatory cytokines are upregulated in obese and insulin-resistant cells. (Kwon and Pessin, 2013). TNF- α mediates insulin resistance by inducing phosphorylation of IRS-1 serine residues by the protein Jun N-Terminal Kinase (JNK). This phosphorylation inhibits IRS-1 and subsequently inhibits downstream receptor tyrosine kinase activity, inhibiting GLUT4 translocation and the remainder of the insulin response (Fig. 1B) (Hotamisligil *et al.*, 1996). TNF- α neutralization or deficiency can decrease insulin-resistance, further exemplifying its role as a disease modulator (Kwon and Pessin, 2013).

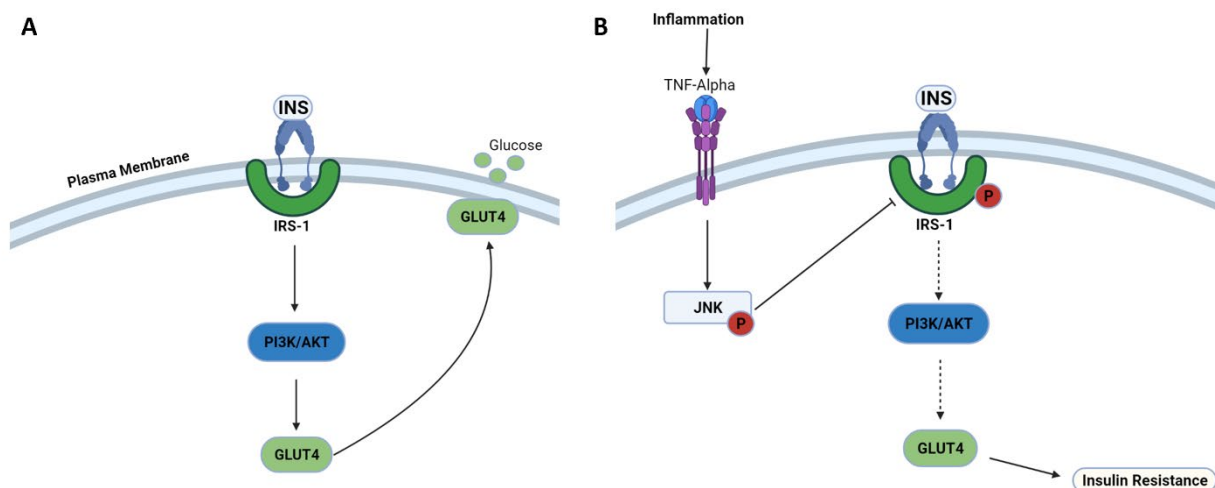


Figure 1: Insulin signaling pathway under normal and insulin-resistant conditions. A) Schematic demonstrating normal insulin signaling activated by the presence of insulin, leading to activation of the PI3K/AKT signaling pathway and glucose release stimulated by glucose GLUT4 translocation to the membrane. B) Release of TNF- α in response inflammation leads to activation of JNK and the subsequent phosphorylation of IRS-1 and the insulin signaling pathway, interrupting GLUT4 translocation and leading to insulin resistance in the cell.

1.3 Modelling insulin resistance to discover potential treatments

Understanding the metabolic contributors to disease is critical for categorizing disease pathology but is also a useful tool for the developing experimental disease models. *In-vitro* disease models are required to study the disease experimentally and discover potential treatments (Lo *et al.*, 2013).

Originally derived from mouse embryonic fibroblast cells, the 3T3-L1 cell line is a pre-adipose tissue line that differentiates to mature adipocytes when stimulated with an adipogenic cocktail. This model is widely used to study insulin resistance in adipocytes (Lo *et al.*, 2013; Green and Meuth, 1974). There are several established ways to induce adipocyte insulin-resistance. Lo *et al.* (2013) investigated five different *in vitro* models of induced insulin resistance in 3T3-L1 cells to determine which model best captured the aspects of *in vivo* insulin resistance: TNF- α , hypoxia, dexamethasone, high insulin, and a combination of TNF- α and hypoxia. When studying markers of insulin signaling pathways, Lo *et al.* (2013) discovered that all five models were able to disrupt PI3K/AKT signaling and result in decreased p-Akt expression, mimicking *in vivo* insulin-resistance (Fig. 1B). Using multiple additional measures of insulin resistance, this study determined that TNF- α or a combination

of TNF- α and hypoxia best mimic the *in vivo* insulin resistance. Specifically, these models capture the downregulation of key metabolic pathways and the upregulation of immune and pro-inflammatory response pathways seen in *in vivo* insulin resistance (Lo *et al.*, 2013). Further, the TNF- α model resulted in decreased GLUT4 expression which is known to be a critical effect of *in vivo* insulin resistance (Fig. 1B). While the model did not perfectly mimic *in vivo* conditions, the presence of the transcriptional insulin-resistance markers indicate that experimental conditions can mimic disease pathology. Thus, researchers can use this model to study diabetes experimentally and to investigate potential treatments (Lo *et al.*, 2013).

In addition to experimental models of disease, discovery of potential disease treatments also requires an understanding of the molecular signaling and communication pathways of the disease modulating hormones. As previously stated, adipocytes are known to secrete many different bioactive substances such as steroids, proteins, peptides, macromolecules, and both pro and anti-inflammatory cytokines (Coelho *et al.*, 2013). In obese adipose tissues, there is a maladaptive secretion of these adipokines, and an unbalanced production of pro-inflammatory cytokines over anti-inflammatory cytokines (Coelho *et al.*, 2013). These secreted molecules function as molecular signals and are detected by cell surface receptors on neighboring and distant cells. TNF- α , IL-6 and chemerin are examples of secreted cytokines upregulated under insulin-resistant conditions (Rabe *et al.*, 2008). Activation of the cognate receptors for these adipokines results in intracellular signal transduction that has diverse roles in the maintenance of energy homeostasis and participates in the pathogenesis of diabetes (Alexandraki *et al.*, 2006; Buechler *et al.*, 2019). The study reported herein is particularly interested in the role of the G-protein coupled receptor (GPCR) family and their potential role in detecting adipokines involved in the disease pathogenesis of type II diabetes. An example of such a connection is the adipokine chemerin, the endogenous agonist of chemerin receptor 1 (CMKLR1) and GPR1. The activation of both GPR1 and CMKLR1 modulates the functions of chemerin; energy homeostasis, and adipogenesis, and both receptors have been connected to the pathogenesis of obesity and type II diabetes (Rourke *et al.*, 2014). This review will now focus on GPCR signaling mechanisms, and a method for detection of GPCR activation.

1.4 G Protein Coupled Receptors

Signal transduction is dependent on the transmission of an extracellular signal from the signalling molecule, the ligand, to the cellular receptor (Heldin *et al.*, 2016). Ligands will act as either agonists, to activate the target receptor, or as antagonists by inhibiting the action of the endogenous ligand, and preventing receptor activation (Brogi *et al.*, 2014). Cell surface receptors, or transmembrane receptors, are embedded in the plasma membrane, and respond to extracellular ligands that are too large to cross the membrane and enter the cell, such as hormones or neurotransmitters (Jensen and Spalding, 2004). The binding of the extracellular ligand to the transmembrane receptor will elicit an intracellular cascade, resulting in programmed changes in gene expression upon reaching the intracellular target (Jensen and Spalding, 2004).

GPCRs are both the largest subfamily of cell-surface receptors, as well as the most abundant therapeutic targets (Rosenbaum *et al.*, 2009). Structurally, all GPCRs, also known as seven-transmembrane (7TM) receptors, have seven transmembrane α -helices, interspersed by extracellular and intracellular loops, with an extracellular N-terminus and an intracellular C-terminus (Fig. 2; Gurevich and Gurevich, 2019). There are five main families of GPCRs in vertebrates, divided based on their structural features: rhodopsin, secretin, glutamate, adhesion, and taste 2 receptor families (Rosenbaum *et al.*, 2009). Most GPCRs share a common mechanism of action, where ligand receptor binding causes a conformation change in the receptor to initiate signal transduction via activation of heterotrimeric G proteins (Rosenbaum *et al.*, 2009). Heterotrimeric G-proteins contain α , β and γ subunits (Fig. 2A). GPCR conformation change, initiated by ligand-binding, allows the receptor to act as a guanine nucleotide exchange factor (GEF), modulating the exchange of Guanosine Diphosphate (GDP) for Guanosine Triphosphate (GTP) at the $G\alpha$ subunit (Fig. 2A; Oldham and Hamm, 2008)). This activates the G protein, causing the subsequent separation of the heterotrimeric protein, and activating downstream signaling targets (Oldham and Hamm, 2008). The structural rearrangement at the $G\alpha$ subunit and its subsequent GTPase action is a critical portion of controlling this activation sequence. Regulators of G Protein signaling (RGS proteins), that stabilize the $G\alpha$ subunits for GTPase activity, also play a critical role in receptor activation (Kimple *et al.*, 2011).

G-protein coupled receptor kinases (GRKs) and arrestins regulate termination of GPCR mediated signaling (Feng *et al.*, 2011). Ligand binding triggers GPCR activation, leading to phosphorylation on serine and threonine residues by GRKs, triggering the GPCR desensitization process and increasing their affinity for arrestins (Luttrell and Lefkowitz, 2002). The subsequent recruitment and binding of the arrestin protein to the GPCR leads to GPCR desensitization, uncoupling the receptor from the G-protein (Walther and Ferguson, 2013). This protects the GPCRs from overstimulation and prolonged agonist exposure, and in turn terminates G-protein dependent signal transduction (Luttrell and Lefkowitz, 2002; Walther and Ferguson, 2013). Internalization, or receptor sequestration, is the second major process that must occur in GPCR signaling, allowing receptors to avoid long term desensitization and leads to receptor recycling and downregulation (Luttrell and Lefkowitz, 2002). β -arrestins are scaffold and adaptor proteins, recruiting the receptors from the plasma membrane to the intracellular space (Walther and Ferguson, 2013). In recruiting the receptors, β -arrestins coordinate their uncoupling from G-proteins, and lead them through clathrin-coated endocytic machinery, containing clathrin, β -adaptin, and the adaptor protein complex AP-2 (Walther and Ferguson, 2013). The sequestered GPCRs can then undergo dephosphorylation, resensitization and recycling back to the plasma membrane, while also in some cases activating G-protein independent signaling pathways (Walther and Ferguson, 2013).

While post-phosphorylation β -arrestin binding clearly facilitates the endocytosis of GPCRs, the process varies depending on the receptor, and differences within the receptors' C-terminal tails (Luttrell and Lefkowitz, 2002). GPCRs classification is based on C-terminal tail structure, which in class A consist of a rich serine/threonine cluster, that can only transiently bind β -arrestins. Conversely, class B receptors such as V2 vasopressin can recruit both β -arrestin-1 and β -arrestin-2 with high affinity (Walther and Ferguson, 2013). β -arrestin binding is dependent on phosphorylation. The C-terminal tails of class B receptors are longer, increasing the number of phosphorylation sites, thus increasing the stability of the β -arrestin binding complex (Kim and Caron, 2008).

1.5 GPCR's as drug targets

Despite the common mechanism of receptor activation, GPCRs are activated by a diverse range of signaling molecules. Among these signals are proteins, peptides, lipids, ions,

and photons (Black *et al.*, 2016). These diverse signaling molecules and overall G-protein diversity make GPCRs attractive drug targets. In addition to mediating most cellular responses to extracellular ligands, GPCRs control three of the five major senses: olfaction, taste, and vision. Of the 800 known GPCRs, four control ocular processing, five are responsible for specific tastes and approximately 400 receptors are responsible for olfaction in humans (Rosenbaum *et al.*, 2009; Spehr and Munger, 2009). While olfactory receptors play a critical role for the detection of odors and volatile chemicals, researchers have not classified them as drug targets yet (Spehr and Munger, 2009). This leaves over 150 distinct GPCRs with known endogenous ligands to mediate cellular responses in biophysical processes, including endocrinology, metabolism, and neuromodulation (Sriram and Insel, 2018). These receptors make up the largest class of drug targets and are also known as the druggable GPCRs or non-olfactory receptors, and 134 GPCRs presently have Food and Drug Administration (FDA) approved drugs (Sriram and Insel, 2018).

To date there remains 60 GPCRs with no proposed endogenous ligands or known physiological functions (Alexander *et al.*, 2020). These are orphan receptors, a notable receptor family that represents possible drug targets for a wide variety of molecular diseases. Thus, the discovery of their endogenous ligands (deorphanization) is a major focus in pharmacology (Roth and Kroeze, 2015). The development of techniques to study orphan GPCRs and their potential deorphanization is widely based on the discovery of β -arrestin recruitment after GPCR activation, independent of G-proteins (Lefkowitz and Shenoy, 2005). These techniques are critical in the development of potential treatments for multiple diseases including obesity and diabetes.

1.6 Measuring GPCR activation: The Tango assay

The rapid responses to cues required for the function of signaling systems makes monitoring protein interactions a challenging task, as most assays require a slower and elucidated response to monitor. Barnea *et al.* (2008), aimed to monitor intracellular protein interactions with more selectivity and sensitivity than other methods. Their study focused on the intracellular GPCR: β -arrestin interactions, through the quantification of receptor activity (Barnea *et al.*, 2008). The result of their study was the Tango assay, transforming rapidly evolving signaling events into stable and amplifiable cellular responses. Barnea *et al.* (2008) discovered they were able to use the Tango assay to quantify activation of GPCRs, receptor

tyrosine kinases, and steroid hormone receptors. Activation of the receptors by ligand binding leads to the recruitment of a β -arrestin linked to a tobacco etch virus (TEV) protease, which cleaves the modified receptor at its C-Terminal tail (Fig. 2B). Modifications to the receptor include a TEV protease cleavage site, and tetracycline transactivator (tTA) sequence on the cytoplasmic C-terminus. Upon cleavage, the receptor releases tTA, translocating it to the nucleus of the cell, where it activates the tTA dependent reporter gene introduced into the cell along with the fusion genes (Barnea *et al.*, 2008). Activation of the reporter gene produces a quantitative measure of GPCR: β -arrestin interactions in stable and amplifiable readout of luciferase activity (Fig. 2B; Barnea *et al.*, 2008).

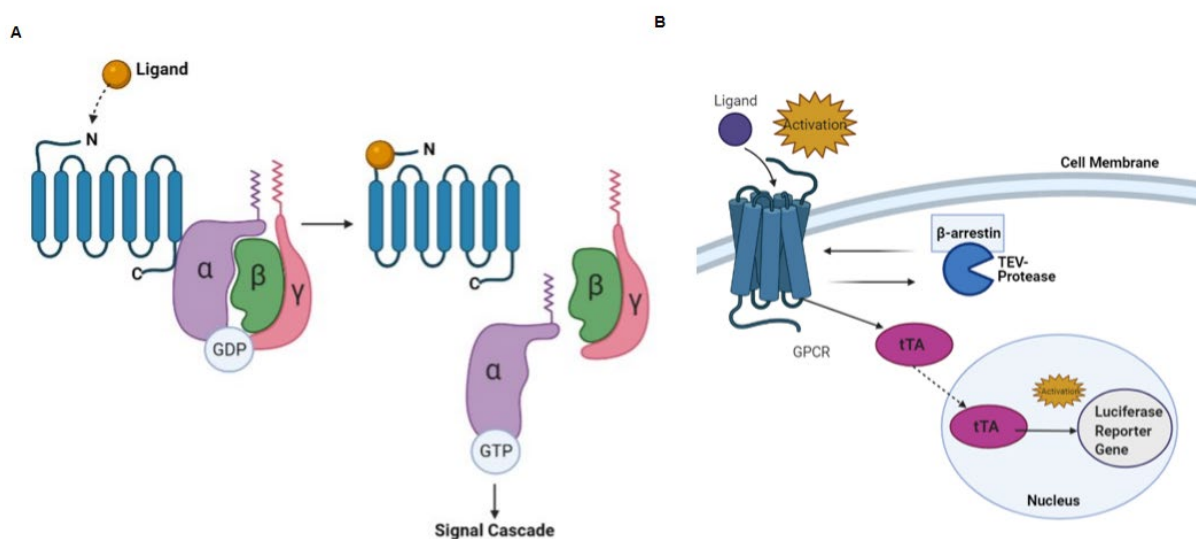


Figure 2: Signal Transduction in the Tango Assay. A) Schematic of typical GPCR activation triggered by ligand binding, leading to a signalling cascade B) GPCR activation in the Tango assay: β -arrestin recruitment triggered by ligand binding receptor activation, leading to tTA translocation and reporter gene activation.

The Tango assay holds many advantages for the quantification of protein interactions, including a stable receptor gene response and quantitative and direct output. Further, the modification of the plasmid DNA molecule to contain the transcription factor eliminates any possible interference from endogenous receptor signaling, since the cell is genetically modified to only respond to the modified tango receptors (Barnea *et al.*, 2008). This assay was applicable to a wide range of receptors because of the nearly ubiquitous use of arrestins following GPCR activation. The sensitivity of the assay to even the slightest changes in

receptor activation allows for constant monitoring of activity at the target receptor, making it suitable for use with orphan GPCRs as a deorphanization method (Barnea *et al.*, 2008). However, there are disadvantages to this method, including a lack of generalizability to the entire GPCRome due to the diversity of signaling pathways, making the method cost and time inefficient for use on high throughput screening protocols (Barnea *et al.*, 2008). Moreover, the method does not allow for the simultaneous screening of different deviants due to the diversity of the signals. In effect, Kroeze *et al.* (2015) developed a secondary method, used for high throughput screening: The Parallel Receptor-ome Expression and Screening *via* Transcriptional Output-Tango (PRESTO-Tango).

1.7 High throughput screening: PRESTO-Tango luciferase assay

To overcome the limitations presented by the Tango assay, Kroeze *et al.* (2015) designed the PRESTO-tango assay to adapt the Tango β -arrestin recruitment assay to the entire druggable GPCRome. This assay allows for rapid and efficient parallel screening of the non-olfactory GPCR family, creating a high throughput screening process. The experimental protocol allowed for screening of biologically active compounds and is a promising approach to investigating orphan GPCRs. Like the Tango assay, the independence from G-protein coupling of the readout signals demonstrated in the PRESTO-Tango makes the approach suitable for identifying potential synthetic and naturally occurring agonists of orphan GPCRs (Kroeze *et al.*, 2015).

While they kept the general concept of the Tango method, Kroeze *et al.* (2015) made adaptations to the efficiency of the method, as well as to the design of the modified plasmid. Modified tango plasmids are accessible to the entire scientific community, adding to the advantages of the PRESTO-tango design (Fig. 3). The 5' end of the plasmid is equipped to promote membrane localization with a hemagglutinin (HA) signal sequence, and cell-surface expression can be monitored by the inclusion of a flag epitope tag (Kroeze *et al.*, 2015). Plasmid design was the same on the 3' end as in Barnea *et al.* (2008), where a TEV-endopeptidase cleavage site and the tTA protein are located at the end of the modified plasmid. The plasmids were further adapted to promote arrestin recruitment, with the inclusion of vasopressin receptor sequences in between GPCR coding sequences and the TEV cleavage site, flanked by restriction sites (Fig. 3; Kroeze *et al.*, 2015). The C-terminal sequence of vasopressin 2 has a high affinity for β -arrestin2, thus promoting arrestin

recruitment for the modified plasmid. The cell line used in this assay is the HTLA cell-line, a modified human embryonic kidney (HEK-293) cell line, stably expressing a tTA-dependent luciferase reporter gene and a β -arrestin2: TEV fusion gene (Fig. 2B; Kroeze *et al.* 2015). The inclusion of the fusion gene promotes and facilitates cleavage. The restriction sites flanking the GPCR coding sequences and the TEV cleavage site add to the overall efficiency of the protocol by promoting easy excision, subcloning and gene synthesis (Kroeze *et al.*, 2015).

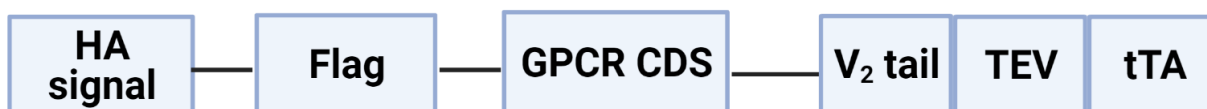


Figure 3: PRESTO-Tango Plasmid. Design of PRESTO-Tango modified plasmid receptor gene. Image adapted from Kroeze *et al.* (2015).

1.8 Adipokines as GPCR ligands

Adipokines are the disease modulating hormones of diabetes and obesity and serve as markers of disease severity. Several adipokines are already classified as GPCR ligands including those involved and upregulated in obesity, such as chemerin, acting as a ligand for the receptor CMKLR1 or and CXCR2 being classified as a chemokine receptor (Poeta *et al.*, 2019; Rourke *et al.*, 2015). Thus, there is evidence for a broader connection between disease modulating adipokines in obesity and diabetes and orphan GPCRs, a connection that would identify potential drug targets and treatments for obesity and type II diabetes.

1.9 Summary and Scope of Study

The aim of this study was to determine if orphan human GPCRs, those for which there are no known endogenous ligands, are adipokine-sensing receptors with the ability to detect molecular differences between healthy and unhealthy adipocytes. This was accomplished through comparison of changes in activation of receptors treated with healthy or insulin resistant adipocyte-conditioned media. It was expected that of the 71 included orphan receptors, there would have been isolated receptors of interest that were activated in response to treatment with either adipocyte-conditioned media or that were differentially activated in response to treatment with insulin-resistant adipocyte-conditioned medium as compared to treatment with healthy adipocyte-conditioned medium.

2. Materials and Methods

2.1 Cell culture

HTLA cells were used for all experiments. These are human embryonic kidney cells, derivative of the HEK-293 line, expressing a stably transfected tetracycline transactivator (tTA) dependent luciferase reporter and β -arrestin2-Tobacco etch virus (TEV) fusion gene (Barnea *et al.*, 2008; Kroeze *et al.*, 2015). Cells were grown at 37°C and 5% CO₂ and kept in complete medium (high glucose (4.5g/L) Dulbecco's Modified Eagle Medium (DMEM; Corning, 10-013-CV) with 10% Fetal Bovine Serum (FBS; Wisent Bioproducts, 243K18), 0.1 mg/mL hygromycin B (Bioshop, 8G55969) and 2 mg/mL puromycin (Bioshop, PUR333.100). Cells were grown to 70% confluency before subculturing and grown to 40-60% confluency before plating in the PRESTO-Tango assay.

2.2 DNA purification

Plasmid DNA for receptor expression vectors were transformed into DH5 α *Escherichia Coli*, and grown on Lysogeny Broth (LB) agar plates (Tryptone 10g/L, Yeast extract 5g/L, Sodium Chloride 5g/L, Agar 15g/L; (Bioshop, LBL406.1)) with 100 μ g/mL ampicillin (Fisher Scientific, BP1760-5) for 18-24 hours at 37°C. Single colonies were inoculated in 100 μ g/mL ampicillin LB broth (Bioshop, LBL405) and allowed to grow for 18-24 hours at 37°C with shaking at 250 rpm. The subsequent DNA purification and extraction was done with Nucleospin Plasmid Transfection-grade mini prep kit (Macherey-Nagel, 74090.250). PCMV- β galactosidase (β -gal), and pBSK (empty vector) were gifts from Sinal CJ (Rourke *et al.*, 2015). All PRESTO-Tango GPCR expression vectors were obtained from Addgene (Roth Lab, Addgene Kit #1000000068) as in Kroeze *et al.* (2015).

2.3 Treatment preparation: Adipocyte-conditioned media

Adipocyte-conditioned medium was prepared in the Sinal Lab at Dalhousie University, as described previously (Lo *et al.*, 2013). 3T3-L1 cells (pre-adipocytes) were treated with complete differentiation media to prepare differentiated 3T3-L1 adipocytes. After differentiation, one group of cells (insulin-resistant) was treated with 2.5 nM TNF- α (Biotechne, 410-MT-010/CF) in MEM-alpha medium, while the rest of the adipocytes (designated as healthy) were treated with MEM-alpha in the absence of TNF- α . Treating the adipocytes with TNF- α induced insulin resistance as evidenced in Appendix 1 and created the insulin-resistant treatment for use in the high throughput screen (HTS). Unconditioned MEM- α complete differentiation medium was used as vehicle (VEH) control.

2.4 PRESTO TANGO assay

The experimental timeline of the PRESTO-Tango assay is outlined in Figure 4.

2.4.1 Plating

Cells were washed with serum free DMEM (Corning, 10-013-CV). and released from the plate by using 0.25% trypsin containing 2.21 mM Ethylenediaminetetraacetic acid (EDTA; Wisent Bioproducts, 325-043 EL). Subsequently, cells were collected by centrifugation for 5 min at 300 x g. In a 96 well plate, cells were plated at 10,000 cells/well in 100 μ L of DMEM containing 5% FBS. To allow for attachment and prepare for transfection, cells were incubated at 37°C and 5% CO₂ for 24 hours.

2.4.2 Transfection

HTLA cells were transiently transfected with a transfection mixture containing 50 ng/well pBSK, 25 ng/well pCMV- β -gal, and either 25 ng/well of Lysophosphatidic Acid Receptor (LPAR1), one of the 71 orphan GPCRs, one of four known adipokine receptors, or pBSK for negative control. A transfection mixture was prepared with this DNA in Opti-MEM with 0.02 mg/mL polyethyleneimine (PEI), and incubated for 15 minutes before a 1:5 dilution in Opti-MEM. In advance of transfection, 70 μ L of media was removed from each well and replaced with 50 μ L of the prepared transfection solutions. Cells were incubated for a maximum of 18 hours at 37°C and 5% CO₂.

2.4.3 Treatment and lysis

Prior to addition of 20 μ L of concentrated treatments, 30 μ L of media was removed from each well. Treatments used for different experiments were as follows: adipocyte-conditioned media; prepared as previously described, MEM-alpha complete differentiation medium, Lysophosphatidic Acid (LPA; VWR, 89160-532) prepared in DiMethyl Sulfoxide (DMSO) to 500 μ M and subsequently diluted in Opti-MEM, TNF- α (Biotechne, 410-MT-010/CF), prepared to 100 μ g/mL and diluted in Opti-MEM, and Opti-MEM for negative control wells. Each plate contained triplicate LPAR1-expressing HTLA cells treated with Opti-MEM and 10% FBS in Opti-MEM. After a 24-hr incubation period at 37°C and 5% CO₂, all media was removed prior to the addition of 20 μ L of 1X Firefly lysis buffer (Biotium, Cat# 99923) and freezing of cells at -80°C.

2.4.4 Luciferase and β -gal assays

Cell lysate was thawed at room temperature, diluted 1:10 in Milli-Q water and resuspended on a microplate shaker for 2 minutes. β -gal assays were performed in 96-well

plates, incubating 30 μL of 2X β -gal assay buffer (0.1 M sodium phosphate buffer (pH 7.3), 1 mM MgCl_2 , 0.067% (w/v) ortho-nitrophenyl- β -galactosidase (ONPG), 50 mM β -mercaptoethanol) with cell lysate for 10 minutes. Subsequently, absorbance was read at 420 nm (A420) using a BioTek Synergy HT luminescence reader and Gen5 software. Firefly lysis buffer (0.1X) was assayed in triplicate on each plate and subtracted as a blank.

White 384-well plates (Greinerbio-one 781075) were used for luciferase assays. 20 μL of the 1:10 diluted cell lysate was incubated with 0.08 mg/mL D-luciferin (Biotium 9907) in luciferase assay buffer (Biotium, 30028L) for 5 minutes with oscillation. Luminescence measurements were done using a BioTek Synergy HT luminescence reader and Gen5 software. Firefly lysis buffer (0.1X) was used as a blank.

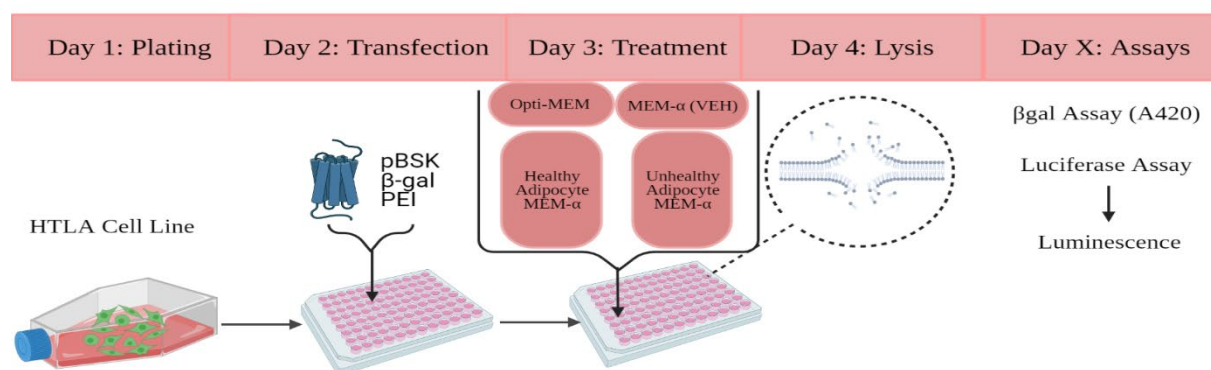


Figure 4: Schematic outlining the experimental timeline of the PRESTO-Tango assay in the HTS experiment. HTLA cells were plated at 10,000 cells/well prior to a 24-hour incubation period, after which they were transfected with pBSK (empty vector), PCMV- β galactosidase (β -gal), and the PRESTO-Tango GPCR of interest using polyethyleneimine (PEI). 18 hours later, cells were treated with Opti-MEM, MEM- α or adipocyte conditioned media and incubated for another 24 hours prior to lysis and storage at -80°C . Receptor activity was then quantified via luciferase and β gal assays.

2.5 Statistical analyses and data transformation

Experiments were performed in biological triplicates denoted as Sets A, B and C, and within each set each experimental condition was measured in triplicate. To account for any differences caused by cell number or receptor expression between wells, the relative luminescence (RLU) measured in each well was divided by the average blank adjusted A420 of the well. A420 adjusted RLU (RLU/A420) of each treatment condition is presented as the average value across the biological replicates, with standard error of the mean. Average fold

change was calculated as compared to the Opti-MEM treatment, by dividing the RLU/A420 of each well by the average RLU/A420 of the receptor's Opti-MEM treatment.

All statistical analyses were performed in Prism 9 (GraphPad Software). For comparisons with more than two groups, the Brown-Forsythe test for homogeneity of variances and Shapiro-Wilk's Test for normality were passed prior to a one-way ANOVA with Holm-Sidak's multiple comparisons. In cases where variances were different, but normality was passed, the Brown-Forsythe ANOVA with multiple comparisons was performed. If data was both abnormal and variances were non-homogenous, Kruskal-Wallis non-parametric ANOVA was performed. Unpaired T-test were used to compare between two groups, along with an F-test for homogeneity of variances and Shapiro-Wilk's test for normality. An α of 0.05 was used for all tests performed. If assumptions failed, Mann-Whitney rank test was used to compare two groups. Finally, for receptor-agonist dose response curves, treatment concentration values were log₁₀ transformed and non-linear fit regression models were applied, from which experimental half maximal effective concentration (EC₅₀) values were calculated.

3. Results

3.1 LPAR1 acts as a control for assay quality

This study used the PRESTO TANGO β -arrestin recruitment assay to study signaling of orphan GPCRS as well as five GPCRs with known agonists in a high throughput screen (HTS). Lysophosphatidic acid receptor (LPAR1) was chosen to function as a control for cell health and assay function in this study because it is a documented class A GPCR (Fig. 5). Treatment of HTLA cells transfected with LPAR1 with the endogenous ligand LPA resulted in a dose dependent activation of LPAR1 in both RLU/A420 and fold-change up to 10-fold (Fig. 5 A-B). The dose-response curve was fit to a linear regression model with a calculated EC₅₀ of 2.28E-06 M, 10-fold higher than the literature EC₅₀ value of 4.00E-07 M (Ruisanchez *et al.*, 2014). HTLA cells transfected with LPAR1 also show significant activation when treated with medium containing FBS, which contains LPA (Fig. 5 C-D). Therefore, treatment of LPAR1 transfected cells with FBS was used as a control for assay quality in the HTS.

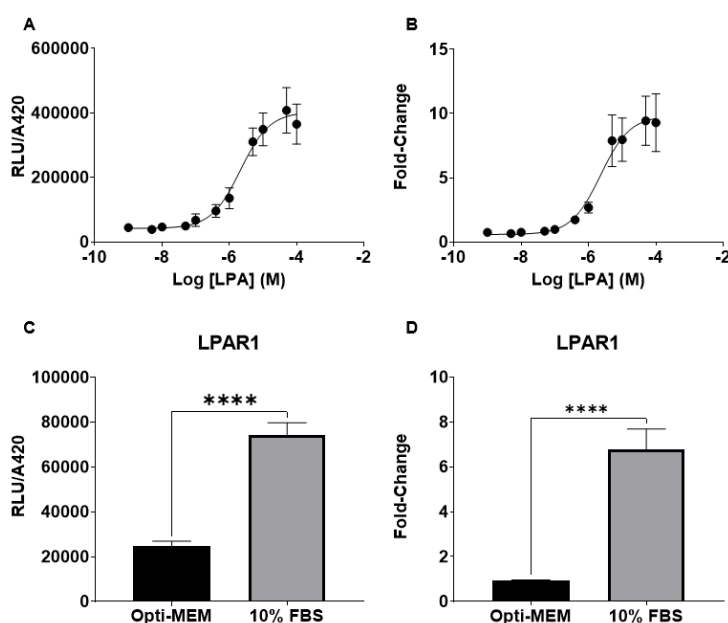


Figure 5: Significant and dose dependent activation of LPAR1-transfected cells upon treatment with endogenous ligand LPA allows LPAR1 to act as a control for assay quality. Activation of LPAR1 was quantified following a β -arrestin recruitment assay in which HTLA cells were transiently transfected with the receptor. A) The Relative Luminescence units (RLU) adjusted by β -galactosidase expression (A420; RLU/A420) of LPAR1 receptor-transfected cells versus log₁₀ treatment concentration of LPA. B) The RLU/A420 Fold-Change data for A. C) The RLU/A420 of LPAR1 transfected cells after treatment with Opti-MEM and LPA containing 10% Fetal Bovine Serum (FBS) in Opti-Mem. D) The RLU/A420 Fold-Change data for C. All data is presented as mean with SEM across three biological replicates. Non-linear regression fit models were applied in Prism to A and B, from which an experimental EC₅₀ of 2.28E-07 M was calculated. ****p<0.0001.

3.2 Adipocyte-conditioned media activates known adipokine receptors

To assess whether adipocyte-conditioned media contents could activate established receptors with known endogenous ligands, five de-orphanized receptors were used as positive controls in the HTS: LPAR1, atypical chemokine receptor 3 (ACKR3), chemerin receptor 1 (CMKLR1), C-X-C Motif Chemokine Receptor 2 (CXCR2), and free fatty acid receptor 1 (FFAR1). HTLA cells transfected with the five positive control receptors were treated with Opti-MEM, Mem- α media (vehicle), healthy adipocyte-conditioned medium (healthy), and insulin-resistant adipocyte-conditioned-medium (insulin-resistant) in the HTS (Fig. 6). Compared to Opti-MEM and vehicle, both healthy and insulin-resistant treatments resulted in significantly increased RLU/A420 for LPAR1 and ACKR3 (Fig. 6A). Further, insulin-resistant treatment significantly increased the RLU/A420 for ACKR3 when compared to healthy treatment, while there was no significant difference between these treatments on the

RLU/A420 for LPAR1 (Fig. 6A). LPAR1 showed the highest fold-change compared to Opti-MEM with healthy treatment, at an average of 25.1 ± 8.21 across three sets, as compared to a fold-change relative to Opti-MEM of 7.76 ± 1.30 with insulin-resistant treatment (Fig. 6B). After healthy treatment, ACKR3 had an average fold-change of 5.62 ± 0.564 compared to 22.6 ± 2.82 after insulin-resistant treatment, thus after insulin-resistant treatment, activation was 4-fold higher than under the healthy treatment condition (Fig. 6B).

To assess whether the presence of TNF- α in the insulin-resistant treatment was impacting the differences in receptor activation between treatments, HTLA cells transfected with LPAR1 and ACKR3 were treated in triplicate with 2.5 nM TNF- α in Opti-MEM (Fig. 6C). TNF- α treatment did not significantly alter the RLU/A420 of either receptor compared to Opti-MEM (Fig. 6C). Compared to Opti-MEM, TNF- α treatment resulted in a decrease in activity in ACKR3, with an average fold-change of 0.393 ± 0.07 across three sets, though this was not found to be statistically significant (Fig. 6 C-D). Together with the data from the HTS, this indicates that media components of the healthy and insulin-resistant treatments are altering the activation of LPAR1 and ACKR3, and that the presence of TNF- α in the insulin-resistant medium is not significantly altering receptor activation.

Neither healthy nor insulin-resistant treatments significantly altered the RLU/A420 of CMKLR1, CXCR2 or FFAR1 compared to Opti-MEM or vehicle treatments (Fig. 6E). Of the three receptors, treatment with insulin-resistant conditioned medium increased the activation of CMKLR1 the most, resulting in a fold-change compared to Opti-MEM of 6.38 ± 1.92 , though large this difference was not found to be statistically significant (Fig. 6 E-F). Due to a lack of statistical significance in any observed changes, these three receptors were not chosen for further validation or follow up studies.

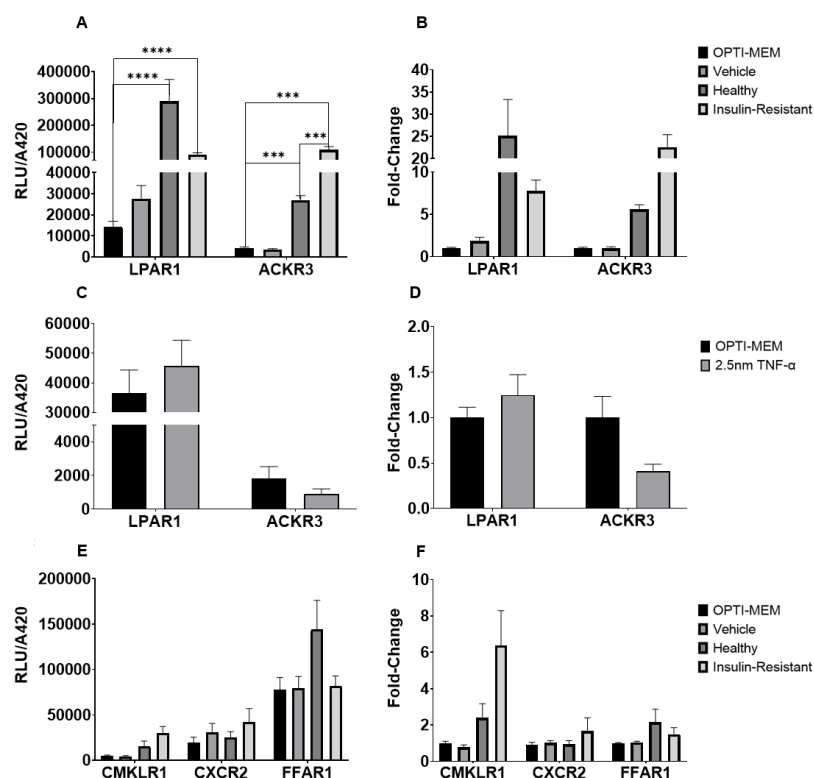


Figure 6: 3T3-L1 adipocyte-conditioned media significantly activates bioactive lipid receptor and atypical chemokine-receptor 3. Receptor activation was quantified following a β -arrestin recruitment assay in which HTLA cells were transiently transfected with GPCRs as indicated. A) The relative luminescence units (RLU) adjusted by β -galactosidase expression (A420; RLU/A420) of HTLA cells transfected with LPAR1 and ACKR3 after treatment with Opti-Mem (black), unconditioned adipocyte differentiation medium (vehicle; light grey), healthy adipocyte-conditioned media (dark grey), and insulin-resistant adipocyte-conditioned media (white). B) The RLU/A420 Fold-Change data from A. C) The RLU/A420 of HTLA cells transfected with LPAR1 after treatment with Opti-MEM or 2.5 nM TNF- α in Opti-MEM. Bar plots are mean with SEM. D) Fold-Change data from C. E) The RLU/A420 of HTLA cells transfected with CMKLR1, CXCR2 or FFAR1 after treatment with Opti-Mem (black), unconditioned adipocyte differentiation medium (vehicle; light grey), healthy adipocyte-conditioned media (dark grey), and insulin-resistant adipocyte-conditioned media (white). F) The RLU/A420 Fold-Change data from C. plots are mean with SEM. **** $p < 0.0001$, *** $p < 0.0005$.

3.3 Orphan receptors differ in basal activation levels

To prepare healthy and insulin-resistant treatments for the HTS, MEM- α adipocyte differentiation medium (vehicle) was conditioned by incubation with healthy or insulin-resistant adipocytes. To assess whether components of the base medium were altering the activity of the receptors, all orphan receptors in the HTS were treated with unconditioned MEM- α or with Opti-MEM, the standard serum-free medium used in the PRESTO TANGO assay (Fig. 7). Compared to treatment with Opti-MEM, treatment with MEM- α did not result

in significantly increased RLU/A420 for any receptor but it resulted in significantly lower RLU/A420 for GPR32 (R37; Fig. 7), indicating that media components were altering GPR32 activation. Thus, for most orphan receptors, treatment with MEM- α did not result in RLU/A420 any different than their baseline activation levels.

There is a notable difference in activation levels across the 71 screened orphan receptors after treatment with Opti-MEM and MEM- α (Fig. 7). While most receptors had a baseline activation in the range of 5000 – 20000, some receptors ranged 20-fold higher than that. Notably, GPR6 (R46) and GPR37 (R39) had the highest levels of basal activation after Opti-MEM treatment, with an average RLU/A420 across three sets of 345964 ± 88329 and 446296.9 ± 85923 , respectively. Their activation levels after vehicle treatment were equally as high, with average RLU/A420 across three sets for GPR6 and GPR7 at 526897 ± 134088 and 484746.3 ± 74516 , respectively (Fig.7). After treatment with Opti-MEM and vehicle, R66 (OPN3) had average RLU/A420 across three sets of 713.588 ± 78.4351 and 780.914 ± 164.595 , respectively, making it the receptor with the lowest basal activity. The data indicates that this set of orphan receptors differ greatly in their basal activation levels.

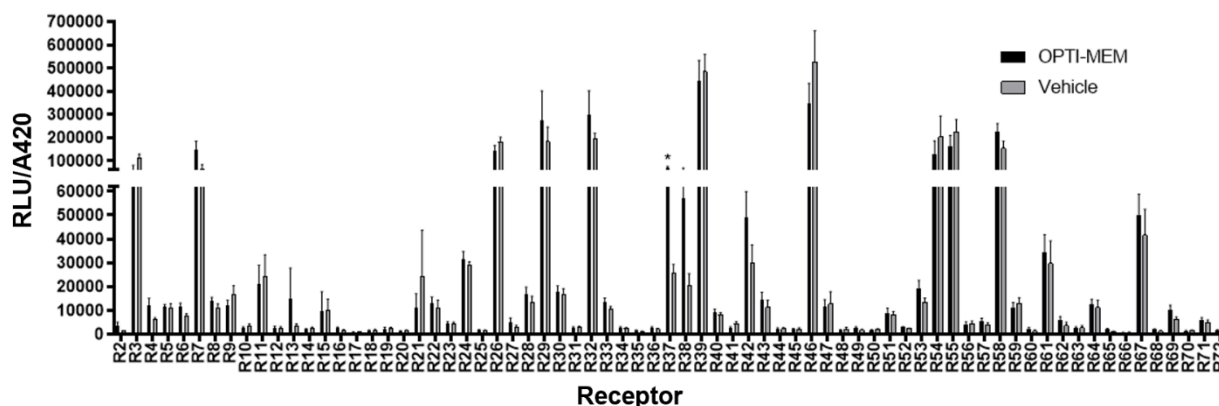


Figure 7: Vehicle treatment significantly decreases RLU/A420 for R37 and orphan GPCRs differ in baseline activation levels. RLU/A420 of cells transfected with 72 orphan receptors after treatment with Opti-MEM (black) or unconditioned adipocyte differentiation medium (vehicle; grey). Data presented as mean with SEM. * $p < 0.0001$.

3.4 Orphan receptors are differentially activated in response to adipocyte-conditioned media

In the HTS experiment, the 71 orphan receptors were differentially activated in response to treatment with adipocyte-conditioned media (Fig.8). While many receptors remained within the range of their baseline activation from Opti-MEM treatment, some

receptors had increased activation after treatment with adipocyte-conditioned-media, and some had decreased levels of activation (Fig. 8). Average fold-change values across three sets between all receptors ranged from 0.1 – 7, with a range of 0.75-1.759 defined as within baseline activation levels (white). Relative to Opti-MEM, treatment with healthy-adipocyte conditioned medium increased the activation of 25 receptors (red) and decreased the activation of 10 receptors (blue), while the remainder of receptors were activated within the range of receptor activation after Opti-MEM treatment. Treatment with insulin-resistant adipocyte-conditioned medium increased the activation of 28 receptors (red) above baseline

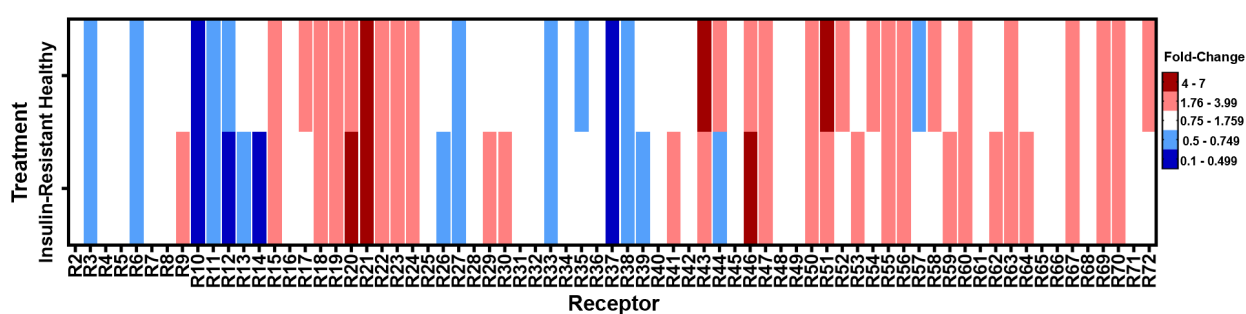


Figure 8: Heat Map of Fold-Change in HTLA cells transfected with 71 orphan receptors following treatment with Healthy or Insulin-Resistant Adipocyte-conditioned media. RLU/A420 fold-change ranging from 0.1-0.499 (dark blue) to 4-7 (dark red) of orphan receptor-transfected cells treated with healthy adipocyte-conditioned media (top) and insulin-resistant adipocyte-conditioned media (bottom). RLU/A420 fold-change is measured relative to RLU/A420 with Opti-MEM treatment. Baseline values (1.76-3.99; white) are representative of the average range of RLU/A420 fold-change of receptors after Opti-MEM treatment.

levels and decreased the activation of 13 receptors (blue).

3.5 Adipocyte-conditioned media significantly alters activation of 19 receptor candidates

Compared to Opti-MEM, treatment with adipocyte conditioned media significantly altered the activation of 19 receptor candidates, significantly increasing the RLU/A420 of 15 receptor candidates and significantly decreasing the activation of four (Fig. 9). The RLU/A420 of 6 receptor candidates (R20, R47, R51, R55, R70, R72) was significantly increased by treatment with either adipocyte conditioned media, while the RLU/A420 of only two receptor candidates (R6 and R37) was significantly decreased by either media (Fig. 9A). The remainder of receptors were significantly altered by only one of either healthy or insulin-resistant adipocyte conditioned media. Of the receptor candidates, GPR153(R21) had the highest biological activation after treatment with both healthy and insulin-resistant

conditioned media, resulting in fold-change values of 6.71 ± 1.08 and 5.35 ± 1.80 , respectively (Fig. 9B). GPR32(R37) was the receptor with the largest decrease in activation after treatment with both media, resulting in fold-change values of 0.190 ± 0.0248 and

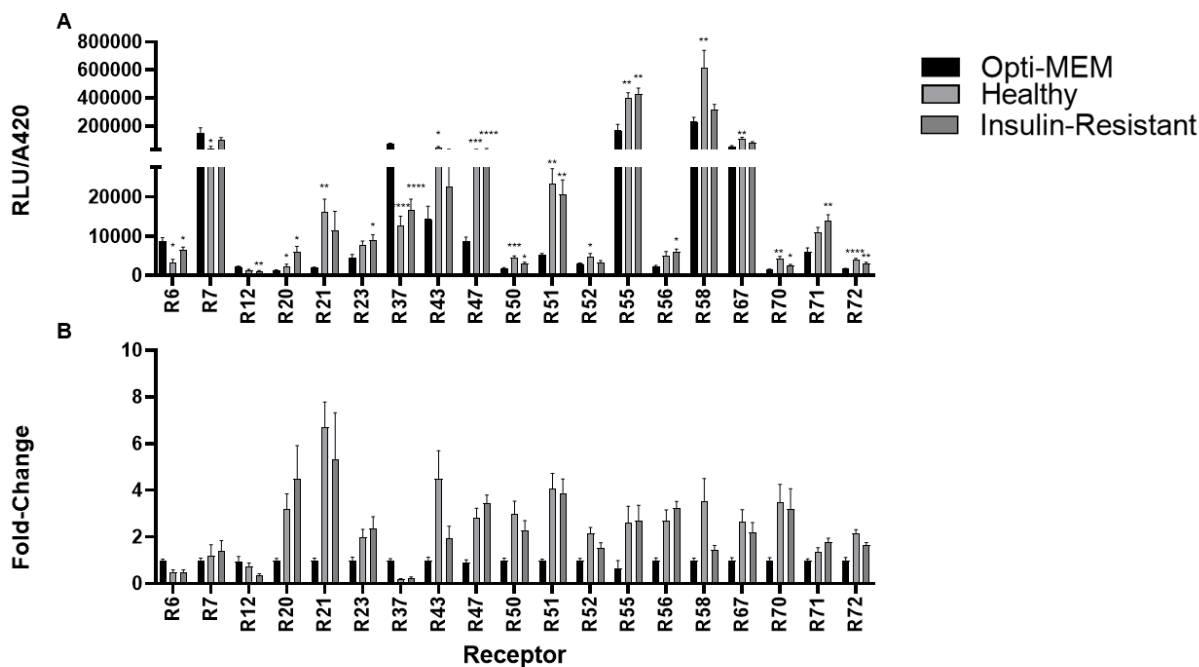


Figure 9: 19 Receptor candidates are significantly and differentially activated in response to adipocyte-conditioned media as compared to controls. Receptor activation was quantified following a β -arrestin recruitment assay in which HTLA cells were transiently transfected with GPCR TANGO plasmids. A) RLU/A420 of GPCR transfected cells whose activity was significantly altered in response to treatment with Healthy Adipocyte Conditioned Media (light grey) and/or Insulin-Resistant Adipocyte Conditioned Media (dark grey) as compared to baseline activation after treatment with Opti-MEM (black). B) The Fold-Change data from A. Data is presented as mean and SEM, * $p < 0.05$, ** $p < 0.005$, *** $p < 0.0005$, **** $p < 0.0001$.

0.244 ± 0.0470 after healthy and insulin-resistant treatment, respectively.

3.6 Insulin-resistant adipocyte-conditioned medium significantly alters receptor activation

For three receptor candidates (GPR17(R26), GPR45(R43) and GPR54(R57)), treatment with insulin-resistant adipocyte conditioned medium resulted in significantly different RLU/A420 compared to treatment with healthy adipocyte-conditioned medium (Fig. 10). Activity of both GPR17 and GPR45 were significantly downregulated compared to treatment with healthy after treatment with insulin-resistant conditioned medium, while GPR54 was the only receptor in which treatment with insulin-resistant adipocyte conditioned

medium resulted in significantly increased activity compared to the healthy treatment (Fig. 10A). GPR54 had the largest fold-change compared to healthy treatment after treatment with insulin-resistant treatment, wherein insulin-resistant medium resulted in a fold-change from Opti-MEM of 3.55 ± 0.95 , nearly 2.5X higher than the fold-change of this receptor after healthy treatment which was 1.44 ± 0.198 (Fig. 10B). Second to this, treatment with insulin-resistant medium resulted in a fold-change of in GPR45, over 2X lower than the fold-change after healthy treatment of 1.93 ± 0.532 . This demonstrates that these receptors are differentially activated in response to insulin-resistant and healthy adipocyte-conditioned media and are sensing molecular differences between the two.

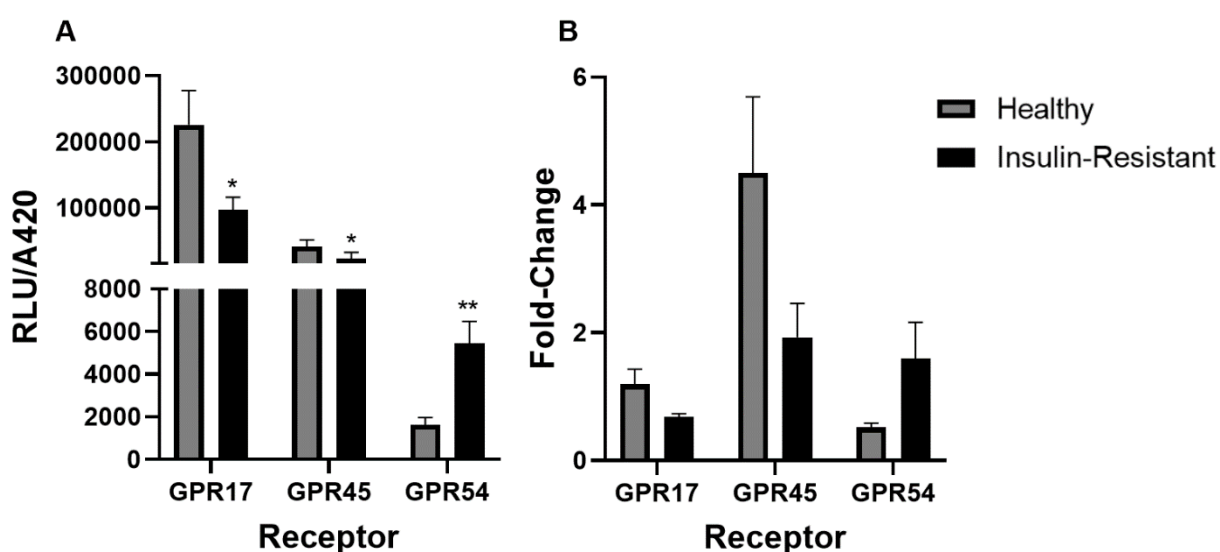


Figure 10: Three receptor candidates are differentially activated in response to treatment with healthy and insulin resistant adipocyte-conditioned media. Receptor activation was quantified following a β -arrestin recruitment assay in which HTLA cells were transiently transfected with GPCR TANGO plasmids. A) RLU/A420 of GPCR TANGO receptors whose activity was significantly altered after treatment of HTLA cells with healthy-adipocyte conditioned media (grey) as compared to treatment with insulin-resistant adipocyte-conditioned media (black). B) RLU/A420 Fold-Change data for A. Fold-Change was measured relative to RLU/A420 of receptor-transfected cells treated with Opti-MEM (Figure 5). Data is presented as mean and SEM, * $p < 0.05$, ** $p < 0.005$, *** $p < 0.0005$.

3.7 TNF- α modulates activation of three receptor candidates

To investigate whether the TNF- α present in the insulin-resistant treatment was acting as an activating or a deactivating molecule for any of the receptors, two of the receptor candidates significantly altered by insulin-resistant conditioned medium (Fig.10) and 10 other

receptors chosen based on preliminary statistical analysis were screened against 2.5nm TNF- α (Fig. 11). GPR54(R57), though significantly altered by insulin-resistant conditioned medium, was excluded from the presented data due to inconclusive results in the screen. Compared to Opti-MEM, treatment with TNF- α significantly increased the RLU/A420 of GPR153 and GPR26 and significantly decreased the RLU/A420 of GPR45 (Fig. 11A). TNF- α treatment did not significantly alter the activation of the remainder of the receptors compared to Opti-MEM. TNF- α treatment had the largest impact on the biological activation of GPR153, resulting in a fold-change of 2.93 ± 1.02 relative to Opti-MEM, and greatly reduced the activation of GPR45 resulting in a fold-change of 0.514 ± 0.182 relative to Opti-MEM (Fig. 11B). Interestingly, activation of GPR17 was significantly increased in response to TNF- α treatment, resulting in a fold-change of 1.69 ± 0.669 relative to Opti-MEM (Fig. 11 A-B). However, insulin-resistant treatment significantly reduced the activation of this receptor compared to healthy treatment, which chose an opposing effect of two treatments containing TNF- α (Fig. 10). Overall, this data indicates that TNF- α can significantly alter the activation of receptors GPR153, GPR17 and GPR45, and that it can both increase and decrease the activation of receptors.

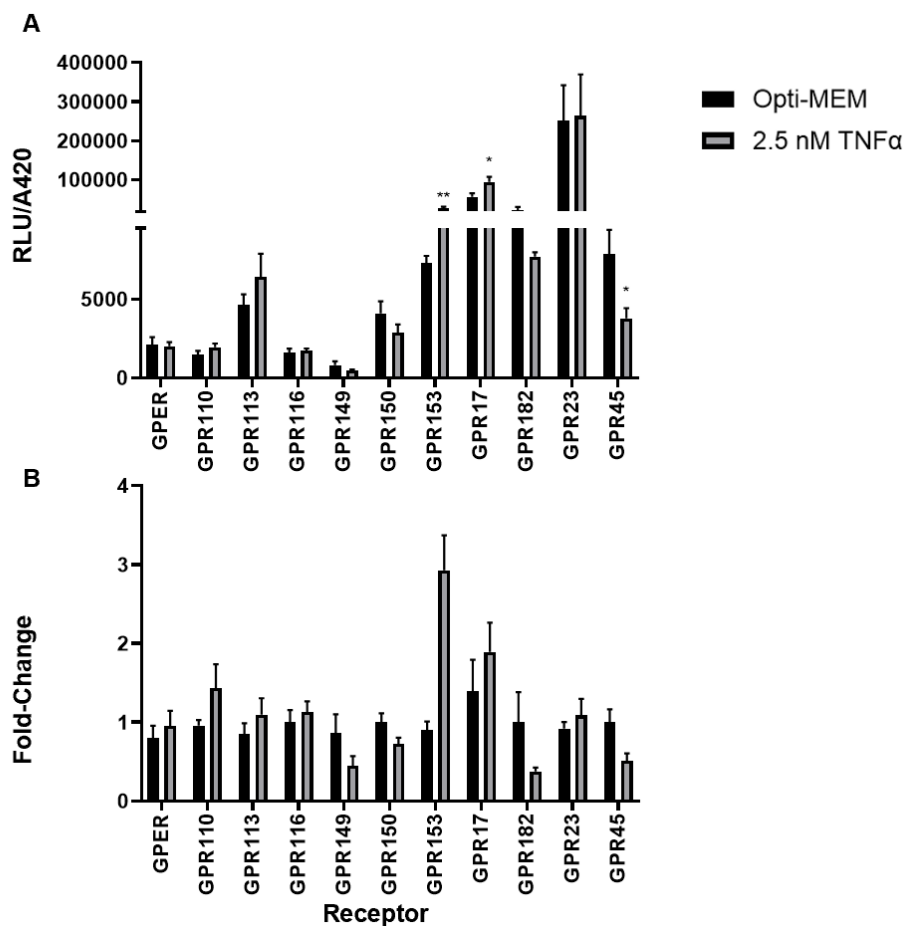


Figure 11: Treatment of receptor transfected HTLA cells with 2.5 nM TNF- α significantly alters the activity of GPR153, GPR45 and GPR17. Receptor activation was quantified following a β -arrestin recruitment assay in which HTLA cells were transiently transfected with GPCR TANGO plasmids. A) RLU/A420 of transfected GPCR TANGO receptors after treatment of HTLA cells with 2.5 nM TNF- α (grey) as compared to treatment with Opti-MEM control (Black) B) RLU/A420 Fold-Change data for A, measured relative to RLU/A420 of receptor-transfected cells treated with Opti-MEM. Data is presented as mean and SEM, *p<0.05, **p<0.005.

3.8 Summary and interpretation of results

Based on all the presented data, receptor candidates whose changes in activation were the most statistically and biologically significant are recommended for validation studies (Table 1). Among the receptors with significantly altered activity between treatment with adipocyte-conditioned media and Opti-MEM (Fig.9) those who had the most notable fold-change levels, both increasing and decreasing, are recommended for validation studies with new samples of adipocyte-conditioned media. These receptors are also recommended for screening against 2.5nm TNF- α to indicate if the presence of this molecule in insulin-resistant medium is contributing to any changes in activation. All receptors that had significantly

altered RLU/A420 after treatment with insulin-resistant adipocyte-conditioned medium (Fig. 10) are recommended for validation studies and to be screened by treatment with TNF- α , if not already done so. Receptors significantly altered by treatment with TNF- α are recommended for dose response curves with TNF- α , one of which was already completed but not included in the data due to inconclusive results (Appendix 3).

Table 1: Interpretation of HTS results: Receptor candidates recommended for further investigation. Fold-Change values relative to Opti-MEM and significance levels (p-values) relative to Opti-MEM of 12 receptor candidates recommended for validation studies after treatment with healthy and insulin-resistant adipocyte-conditioned media in the HTS. p-values between adipocyte-conditioned media treatments for the 12 receptors also presented, as well as p-values from treatment with TNF- α relative to Opti-MEM, if follow up study already completed. *p<0.05

Receptor Number	Receptor Name	Fold-Change Healthy	Fold-Change Insulin-Resistant	P-value healthy vs Opti-MEM	P-value insulin-resistant vs Opti-MEM	P-value Insulin-Resistant vs Healthy	TNF- α test P value or recommendation
R6	GPR116	0.506±0.0902	0.505±0.0879	↓ 0.0432	↓ 0.0432	0.9591	0.6463
R12	GPR142	0.727±0.153	0.379±0.0538	0.382	↓ 0.0064	0.0905	Test Required
R20	GPR151	3.18±0.66	4.48±1.42	↑ 0.0434	↑ 0.0107	0.9693	Test Required
R21	GPR153	6.71±1.08	5.35±1.80	↑0.005	0.201	>0.999	↑ 0.0012
R26	GPR17	1.20±0.234	0.679±0.051	0.213	0.519	↓ 0.0287	↑ 0.0205
R43	GPR45	4.50±1.19	1.93±0.532	↑ 0.0371	0.6816	↓ 0.0255	↓ 0.0287
R47	GPR61	2.84±0.400	3.45±0.343	↑ 0.0001	↑ < 0.0001	0.2602	Test Required
R51	GPR78	4.06±0.659	3.89±0.597	↑ 0.0041	↑ 0.0041	0.9451	Test Required
R55	GPR87	2.62±0.700	2.67±0.691	↑ 0.0047	↑ 0.0073	0.7551	Test Required
R57	GPR54	0.516±0.0665	1.60±0.567	0.0863	0.3778	↑ 0.0071	Test Required
R58	MAS1	3.55±0.953	1.44±0.198	↑ 0.0036	0.5541	0.2243	Test Required
R72	TAAR9	2.15±0.162	1.65±0.113	↑ <0.0001	↑ 0.0057	0.1561	Test Required

4. Discussion

The aim of this study was to determine if healthy and insulin-resistant adipocytes could significantly modulate the activity of orphan GPCRs, and if the molecular differences between healthy and insulin-resistant adipocytes resulted in significantly different levels of GPCR activation. Further, this study also investigated whether adipocyte-conditioned media could significantly alter the activity of already categorized adipokine receptors LPAR1, ACKR3, CMKLR1, FFAR1, and CXCR2. Both healthy and insulin-resistant adipocyte-conditioned media significantly altered the activation of LPAR1 and ACKR3, but not the other three control receptors. Either one or both adipocyte-conditioned media significantly altered the activation of 19 receptor candidates (Fig.9). The treatments significantly increased

the activity of 15 receptor candidates and decreased the activity of the remaining 4. Of these 19 receptors, some receptors were significantly altered by both adipocyte treatments, whereas others were only impacted by one or the other. Finally, compared to healthy adipocyte-conditioned medium, insulin-resistant adipocyte conditioned medium significantly decreased the activation of GPR17 and GPR45 and significantly increased the activation of GPR54. Of these significantly altered receptors, 12 receptors were recommended for follow up studies. Altogether, this study provides evidence that components of both healthy and insulin-resistant adipocyte-conditioned media can significantly alter the activation of orphan GPCRs, and that some receptors can modulate the molecular differences between the two. Thus, there is evidence for a connection between these disease modulating hormones of type II diabetes and orphan GPCRs.

4.1 Adipocyte-conditioned media contains endogenous ligands LPA and ACKR3

The PRESTO-Tango assay measures receptor activity in terms of β -arrestin recruitment (Kroeze *et al.*, 2015). The recruitment of a β -arrestin-TEV protease to the activated GPCR-TEV cleavage site-tTA fusion protein results in the release of tTA that travels to the nucleus and results in an increase of luciferase expression (Kroeze *et al.*, 2015). Increased RLU/A420 corresponds to this increase of luciferase expression resulting from GPCR activation. Thus, the significant increase in RLU/A420 of adipocyte-conditioned-media treated LPAR1- and ACKR3-expressing cells, compared to Opti-MEM, indicates that components of the media are acting as agonists, to increase receptor activation (Fig. 6). This is further supported in that treatment of LPAR1-transfected cells with LPA and with serum containing LPA significantly increased the RLU/A420 of LPAR1 compared to Opti-MEM treatment, confirming the function of this Tango assay (Fig. 5). Where both LPAR1 and ACKR3 have classified endogenous ligands, this further indicates that their endogenous ligands are present in the adipocyte-conditioned media.

LPAR1 is a classified receptor for LPA, the bioactive lipid (Fukushima and Chun, 2001). Thus, the significant increase in RLU/A420 of adipocyte-conditioned media treated LPAR1-expressing cells indicates that LPA is present in these treatments, acting as an agonist to LPAR1. This is further supported by studies showing that adipocytes secrete LPA *in vivo* (Gesta *et al.*, 2002). However, it is more difficult to explain why LPAR1-expressing cells had higher RLU/A420 after treatment with healthy medium as opposed to insulin-

resistant (Fig. 6A-B). Studies indicate plasma LPA levels increase under obese conditions and in insulin-resistant models, which would indicate that LPA levels, and thus the activation of LPAR1, should be higher after treatment with insulin-resistant adipocyte-conditioned medium (D'Souza *et al.*, 2018). However, where the differences caused by the two adipocyte-conditioned media were not significant, further investigation and follow up studies will help to clarify what is causing this change. Overall, the data indicates that LPA is clearly present in both adipocyte-conditioned media, and results in increased receptor activation.

ACKR3 is a recently deorphanized receptor now classified as a chemokine receptor with endogenous ligands C-X-C motif chemokine ligand 12 (CXCL12) and C-X-C motif chemokine ligand 11 (CXCL11). Gene expression analyses have indicated that the expression of the stromal derived factor (SDF)-1 gene, which codes for CXCL12, is higher in adipocytes under insulin-desensitized conditions than under healthy conditions (Shin *et al.*, 2018). Shin *et al.* (2018) demonstrated that adipocytes with TNF- α induced insulin-resistance, like the model used in this study, correlated to a 3.5-fold higher expression of SDF-1 and CXCL12 than found in control adipocytes. In this study, treating ACKR3-expressing cells with insulin-resistant adipocyte-conditioned medium resulted in a significantly increased RLU/A420 compared to treatment with healthy adipocyte-conditioned medium (Fig. 6A-B). A potential model for explaining this result is that overall expression of CXCL12, which is known to positively correlate with ACKR3, is effecting the activation of the receptor (Janssens *et al.*, 2018). However, the data also indicate that CXCL12 is present in the healthy adipocyte-conditioned media, albeit at a lower amount than in the insulin-resistant treatment, resulting in lower levels of receptor activation. This is supported by studies that show CXCL12 expression in both healthy and insulin-resistant 3T3-L1 adipocytes (Shin *et al.*, 2018). Overall, these findings indicate the presence of CXCL12 in the media and that the adipocytes are secreting adipokines into the conditioned media as hypothesized.

4.2 Categorizing receptor activation

Twelve receptor candidates significantly altered by adipocyte-conditioned media treatments (GPR116(R6), GPR142(R12), GPR151(R20), GPR153(R21), GPR26(R17), GPR45(R43), GPR61(R47), GPR78(R51), GPR87(R55), GPR54(R57), MAS1(R58), TAAR9(R72)), were recommended for further characterization and validation studies based

on their significant activation and notable fold-changes (Table 1). To present models to explain their responses, these receptors can be divided into the following categories: 1) Receptors that were activated by both adipocyte-conditioned media treatments, 2) Receptors that had decreased activation in response to both adipocyte-conditioned media treatments and 3) Receptors that were differentially activated by insulin-resistant adipocyte-conditioned medium compared to healthy adipocyte-conditioned medium. This review will now focus on summarizing what is known about these orphan receptors, and to put forth models to explain their responses to the adipocyte-conditioned media treatments.

4.3 Receptors that were activated by both treatments

Five receptors had significantly increased RLU/A420 in response to treatment with both adipocyte-conditioned media: GPR151, GPR61, GPR78, GPR87, and TAAR9 (Fig. 9). As previously described, an increase in RLU/A420 results from an increase in luciferase expression due to GPCR activation. This demonstrates that these GPCRs are signaling in response to the binding of an agonist. Where this extent of GPCR activation was absent in Opti-MEM and VEH treatment for these receptors, there is evidently a component of the adipocyte-conditioned media, something secreted from the adipocytes into the media, that is acting to induce this receptor activation. In other words, it appears as though unidentified secreted adipokines are acting as agonists to these receptors causing an increase in their activation relative to basal activation. The characterization of these activated receptor candidates varies greatly and will each be described separately, though the characterization of several of these receptors remains elusive.

4.3.1 GPR151

GPR151 is a class A orphan receptor and is primarily expressed in the nervous system, and has recently been discovered to be particularly expressed in the habenula in the dorsal thalamus of both rodent and human brains (Antolin-Fontes *et al.*, 2020). GPR151 is a modulator of habenular function and plays a role in the control of addiction vulnerability. Some of the earliest classifications of GPR151 identified its sequence homology to the family of galanin receptors (Holmes *et al.*, 2017). However, galanin has not been identified as an endogenous ligand of GPR151 due to only inducing low levels of activation (EC₅₀ of 2 μ M) and inconsistency of recreating these findings (Holmes *et al.*, 2017). However, since GPR151 was activated in response to galanin, it has been proposed that the unidentified

endogenous ligand of GPR151 may share structural features with galanin, a neuropeptide. Therefore, while its endogenous ligand has not yet been identified, there are some structural features to look for in identifying a cognate ligand for GPR151, which may be a protein.

Activation of GPR151-expressing cells was significantly increased after treatment with both adipocyte-conditioned media; thus, the potential activating molecule must be secreted by adipocytes in both healthy and insulin-resistant conditions. Adipocytes secrete a wide variety of bioactive substances, such as hormones, growth factors and cytokines (Coelho *et al.*, 2013). Adipocytes can also secrete some neuropeptides, and it has been demonstrated that human adipose tissues can secrete the central orexigenic neuropeptide Y (NPY), which plays a role in obesity and appetite regulation (Kos *et al.*, 2007). Where the proposed endogenous ligand of GPR151 likely shares structural features with galanin, it likely to be another neuropeptide, and NPY is similar in structure and size to galanin. Therefore, it is plausible that a neuropeptide secreted by adipose tissue, like NPY, is an agonist for GPR151. The significantly increased RLU/A420 of GPR151-expressing cells after treatment with both media indicates the secreted neuropeptide must be secreted under both healthy and insulin-resistant conditions. Analysis of the components of the media will identify if any neuropeptides are present, and if they share structural similarities to galanin they should be assessed as potential agonists for GPR151.

4.3.2 GPR61

Currently, little is known about the elusive orphan receptor GPR61. GPR61 is mainly expressed in the brain though can be found in other cells around the body, such as the pancreatic β -cells (Oishi *et al.*, 2017). Rodent studies have revealed that mice lacking GPR61 are obese and hyperphagic, categorizing the potential role of this receptor in appetite regulation, energy homeostasis and obesity (Oishi *et al.*, 2017). At this time, GPR61 has no proposed synthetic or endogenous ligands, however several studies have investigated the constitutive activity of GPR61. Oishi *et al.* (2017) demonstrated that GPR61 could recruit β -arrestin in an agonist-independent mode, indicating the constitutive activity of this receptor, and indicating that the resulting luciferase activity in GPR61-expressing cells in this study could be agonist-independent. However, this would not explain the significant increase in expression of GPR61-expressing cells relative to Opti-MEM after healthy and insulin-resistant adipocyte-conditioned media treatments of 2.84- and 3.45-fold, respectively. This

notable increase indicates the presence of an agonist. Again, with little known about potential endogenous ligands for GPR61, this is a difficult agonist to identify. Yet, the role of GPR61 in energy homeostasis and obesity positions it well to respond to secretions from adipose tissue that regulate these same processes. Thus, we propose that an unknown secretion from both healthy and insulin-resistant adipose tissue is acting through endocrine mechanisms to act on GPR61 in either the brain or the pancreas, resulting in its significantly increased activation.

4.3.3 GPR78

GPR78 is another elusive receptor, with little information presented about its potential agonists. GPR78 is expressed in the pituitary and throughout the placenta and is thought to be an important receptor for modulating psychiatric diseases such as bipolar disorder and schizophrenia (Khan and He, 2017). GPR78 is a class A orphan receptor and part of a structurally related (51% sequence identity) family of constitutively active receptors with GPR26. Being constitutively active, GPR78 can exert its downstream effects, like the activation of cyclic adenosine monophosphate (cAMP), without the presence of an agonist (Khan and He, 2017). With this, it is plausible that the significant increase in RLU/A420 of GPR78-expressing cells after treatment with both adipocyte-conditioned media was agonist-independent. However, such a notable increase in RLU/A420 from Opti-MEM treatment after healthy adipocyte-conditioned medium (fold-change of 4.06 ± 0.659) and insulin-resistant adipocyte-conditioned medium (fold-change of 3.89 ± 0.597) indicates that there is a signaling molecule increasing the activation of this receptor beyond constitutive activity.

With little is known about this receptor, and no connections are currently found between adipocyte-secreted molecules and GPR78, its significant increase in activation after adipocyte-conditioned media treatment is very intriguing. It is therefore proposed that the increase in RLU/A420 is either agonist independent, or there is a potential agonist being secreted in the adipocyte-treatments. With little known about GPR78's potential agonists, and so many diverse secretions from adipocytes, proposing an identity for this unknown agonist is quite difficult. Future studies that identify the components of the media will aid in potentially discovering the identity of endogenous ligands for this receptor.

4.3.4 GPR87

GPR87 is another class A orphan receptor whose function has mainly been linked to tumor progression and is overexpressed in various carcinomas (Zhang *et al.*, 2010). GPR87

shares structural similarities to the LPA receptors, and LPA was proposed as its endogenous ligand (Tabata *et al.*, 2007). No other publications have since proposed other endogenous ligands and GPR87 is now considered an LPA receptor. It was already proposed that LPA is present in both adipocyte-conditioned media, considering the significant increase in RLU/A420 for LPAR1-expressing cells upon treatment (Fig. 6). Further, studies have demonstrated that healthy and insulin-resistant adipose tissues secrete LPA (Gesta *et al.*, 2002). The significant activation of GPR87 further supports this hypothesis and aids to demonstrate that LPA is an agonist of GPR87. However, it should be noted that the increase in expression for LPAR1-expressing cells was much larger than GPR87-expressing cells, indicating an imbalance in how the two react to the same agonist. There are two follow up studies that should be performed to confirm whether LPA is acting as an agonist on GPR87: 1) treat GPR87-expressing cells with 10% FBS in Opti-MEM and see if this significantly increases RLU/A420 relative to Opti-MEM, as in LPAR1-expressing cells (Fig. 5C-D), and 2) perform a receptor-agonist dose response curve with LPA and GPR87 to identify whether the activation is dose-dependent and calculate the EC50 for this receptor-agonist relationship.

4.3.5 TAAR9

Trace amine associated receptors (TAAR) are a subfamily of GPCRs that have become increasingly studied for their therapeutic potential for a wide variety of diseases, specifically neurological disorders (Christian and Berry, 2018). TAAR1 is the most well studied and the only officially deorphanized member of the family, though there are other TAARs with proposed endogenous ligands (Christian and Berry, 2018). TAAR9 however, is one of the least studied members of the receptor family though. TAAR9 expression in humans has been localized to the pituitary gland, skeletal muscle, the spleen and in the full range of human leukocytes (Christian and Berry, 2018). TAAR9 currently has no proposed endogenous ligand, but can be activated by two synthetic agonists, N-methylpiperidine and N, N-dimethylcyclohexylamine (Murtazina *et al.*, 2021). Thus, it is likely that any potent cognate ligand for TAAR9 would share similar structural features to these synthetic tertiary amines.

The significant increase in RLU/A420 of TAAR9-expressing cells in response to adipocyte-conditioned media treatment indicates the presence of an agonist, and as previously stated this agonist is likely to bear structural similarities to the synthetic ligands of

TAAR9. With this, it is possible that the adipocyte-conditioned media produces a small molecule or ion that is similar in structure to an amine and is modulating these changes in receptor activation. Further, the knowledge that TAAR9 is expressed across leukocytes indicates that it has great potential to respond to adipose tissue and mediate inflammatory processes (Christian and Berry, 2018). Identification of the components of the adipocyte-conditioned media to identify if any components are structurally similar to the synthetic ligands for TAAR9 will aid in identifying the endogenous agonist for TAAR9 present in the media.

4.4 Receptors that had decreased activation in response to both treatments

Treatment with both adipocyte-conditioned media resulted in significantly decreased RLU/A420 for GPR116(R6)-expressing cells compared to treatment with Opti-MEM (Fig. 9). Relative to Opti-MEM, treatment with healthy adipocyte-conditioned medium resulted in a fold-change of 0.506 ± 0.0902 and treatment with insulin-resistant adipocyte-conditioned medium attributed to a fold-change of 0.505 ± 0.0879 , meaning that these treatments both nearly halved the basal receptor activity (Table 1). This indicates that there is a molecule secreted by both models of adipocytes that is present in both media decreasing the activation of GPR116 and resulting in lower RLU/A420. Decreases in GPCR signaling are either due to the presence of an inverse agonist, which has the ability to bind a receptor and silence its basal activity, or related to an antagonist, which inhibits activation by preventing agonist binding (Black *et al.*, 2016). GPR116 is an adhesion class receptor, a class of receptor that mostly have classified constitutive activities, receptor activity in the absence of a ligand (Bassilana *et al.*, 2019). Thus, it is most likely that the basal activity level of the receptor in response to treatment with Opti-MEM is due to constitutive activity, not the presence of a ligand, meaning that the decrease in RLU/A420 after treatment with adipocyte-conditioned media is the effect of an unknown inverse agonist present in the media.

GPR116 is dynamically expressed throughout adipose tissue (Suchý *et al.*, 2020). It is also thought to play a role in adipogenesis and adipocyte function (Suchý *et al.*, 2020). Due to this dynamic expression in adipocytes, GPR116 likely plays a critical role in energy homeostasis and would be well positioned to respond to molecular signals from adipokines. It should also be noted that GPR116 did not have significantly decreased RLU/A420 in response to treatment with TNF- α (Fig. 11), indicating that there is another component of the

media secreted by the adipocytes that is regulating the receptor's activation. With this, we propose that an unknown adipokine secreted by both healthy and insulin-resistant adipocytes signals via autocrine mechanisms to GPR116 on adipocytes, and the binding of this ligand decreases receptor activation. Thus, this unknown adipokine is acting as either an antagonist or an inverse agonist to GPR116. As previously mentioned, due to the knowledge that GPR116 likely has constitutive activity leading to the RLU/A420 experienced after Opti-MEM treatment, this unknown adipokine is most likely an inverse agonist. Future studies should focus on identifying these media components and isolating the signaling molecule that is acting as a GPR116 inverse agonist.

It should also be noted that another receptor, GPR32(R37) had significantly decreased RLU/A420 relative to Opti-MEM in response to treatment with both adipocyte-conditioned media (Fig. 9). However, treatment with VEH also resulted in significantly decreased RLU/A420 relative to Opti-MEM (Fig. 7), and thus the decreases in activation were attributed to the MEM- α media and not the adipocytes. GPR32 was therefore excluded from the list of receptors recommended for validation studies.

4.5 Receptors differentially activated between adipocyte-conditioned media treatments

Six receptor candidates were identified as receptors with the potential to modulate the difference between the healthy and insulin-resistant adipocyte-conditioned media. Compared to healthy adipocyte-conditioned medium treatment, treatment with insulin-resistant adipocyte conditioned medium significantly altered the RLU/A420 of GPR17(R26), GPR45(R43) and GPR54(R54)-expressing cells. The other three receptors included in this category, GPR153(R21), GPR142(R12) and MASI(R58) did not have significantly altered RLU/A420 between treatments, but only had significantly altered RLU/A420 relative to Opti-MEM in response to one adipocyte-conditioned medium and not the other. These six receptors are thus regulated by signaling molecules that differ in expression between the healthy and insulin-resistant adipocytes, indicating that there are differences in the molecules secreted in the two media.

4.5.1 GPR17

There are confounding findings presented about the endogenous ligands of GPR17. GPR17 is structurally and phylogenetically related to cysteinyl leukotriene (cysLT) and nucleotide (P2Y) receptors (Davenport *et al.*, 2013). Some studies have proposed that both

cysLTs and uracil nucleotides can activate GPR17 and are thus potential endogenous agonists, though several follow up studies failed to replicate this result (Davenport *et al.*, 2013). This suggests that the endogenous ligand of GPR17 remains undiscovered, and more studies are required to further understand this receptor. GPR17 also has two identified synthetic antagonists: Montelukast and Pranlukast (Hennen *et al.*, 2013).

In this study, compared to Opti-MEM, treatment with adipocyte-conditioned media did not significantly alter the response of GPR17, yet insulin-resistant treatment resulted in a significantly lower RLU/A420 compared to treatment with healthy medium. This indicates the presence of either an antagonist or an inverse agonist to GPR17 in the insulin-resistant adipocyte conditioned medium. Interestingly, treatment with TNF- α significantly activated GPR17, the opposite effect that was hypothesized considering the decrease in activation in response to TNF- α containing insulin-resistant adipocyte-conditioned medium. There exists evidence for a connection between TNF- α and GPR17. Wang *et al.*, (2020) found that GPR17 inhibition by Pranlukast reduced the impact of TNF- α induced collagen loss. With this, they concluded that there was a connection between GPR17 signaling and TNF- α , and further exemplified the impact of the synthetic antagonist Pranlukast on GPR17 signaling (Wang *et al.*, 2020).

We propose that TNF- α is a potential endogenous agonist to GPR17. To explain the decrease in receptor activation after treatment with insulin-resistant adipocyte-conditioned medium, we propose two potential models: 1) the presence of an antagonist to TNF- α blocking it from binding and activating GPR17, an antagonist with similar structural features to the known synthetic antagonist Pranlukast or 2) that TNF- α levels in the medium are not sufficient to activate GPR17, and the downregulation is due to the action of an inverse agonist, only secreted in the insulin-resistant adipocyte-conditioned medium, decreasing its RLU/A420 relative to the healthy adipocyte-conditioned medium. With this second model, it is proposed that the RLU/A420 in response to Opti-MEM and healthy adipocyte-conditioned medium of GPR17-expressing cells and is agonist-independent. This would indicate that the receptor has constitutive activity, a hypothesis that is supported in the literature (Martin *et al.*, 2015). An important follow up study to classify the relationship between TNF- α and GPR17 would be a dose response curve to elucidate this agonist-receptor relationship.

4.5.2 GPR45

Little has been described about potential agonists of GPR45. GPR45 is also a class A orphan, expressed throughout the brain and in the liver (Cui *et al.*, 2016). Recently, GPR45 has been investigated for a potential role in mediating obesity. GPR45 knockout in mice models displayed reduced expression of the metabolic regulator pro-opiomelanocortin (POMC), increased adipose tissue accumulation, fat content, body mass and glucose intolerance (Cui *et al.*, 2016). Where cognate ligands of GPR45 remain unknown, in the least its potential role in obesity has been elucidated, which could be critical in the identification of its agonists.

In this study, RLU/A420 of GPR45-expressing cells was significantly decreased in response to insulin-resistant adipocyte-conditioned medium compared to healthy adipocyte-conditioned medium, indicating the presence of either an antagonist or an inverse agonist of GPR45 in the insulin-resistant adipocyte-conditioned medium. Further, GPR45-expressing cells had increased RLU/A420 after treatment with healthy adipocyte-conditioned medium relative to Opti-MEM, which indicates the presence of an agonist in this medium. This indicates that this agonist is secreted by the healthy adipocytes and not the insulin-resistant adipocytes, or that an antagonist to GPR45 is secreted by the insulin-resistant adipocytes and is blocking the activation by the agonist. However, TNF- α treatment significantly decreased the activation of GPR45, indicating that TNF- α could be an inverse agonist of GPR45, decreasing its constitutive activity, which would indicate the presence of an agonist in the healthy adipocyte-conditioned medium. Little is known about GPR45 ligands; therefore, the identity of this agonist is difficult to identify; however, the role of GPR45 in mediating energy homeostasis supports its regulation by anti-inflammatory adipose secretions (Cui *et al.*, 2016). Performing a TNF- α dose response curve to further understand this relationship will be necessary, as well as media analyses to identify the exact level of TNF- α present.

4.5.3 GPR54

GPR54, also known as kisspeptin receptor 1, is a member of the kisspeptin receptor family as the name aptly suggests. GPR54 is expressed mainly in the pituitary gland and the placenta, and throughout the pancreas, brain, liver, and skeletal muscle, as well as in brown adipose tissue (Wang *et al.*, 2018). Kisspeptin (kp) and its cleavage products including kp-10, kp-13, and kp-14 are the proposed endogenous ligands to GPR54, which have all been found equipotent for activating GPR54 (Davenport *et al.*, 2020). Synthetic kp10 analogues have

been identified as antagonists to GPR54 (Davenport *et al.*, 2020). As its expression pattern suggests, GPR54 is mainly involved in reproduction, with a critical role at the nervous-gonadal axis (Wang *et al.*, 2018). However, GPR54 has been more recently described for action in modulating energy metabolism (Tolson *et al.*, 2020). Endogenous kisspeptin signaling in adipose tissue was first identified in a study by Tolson *et al.* (2020), where GPR54 knock out mice experienced lowered body weight and higher metabolic rate, elucidating the role of GPR54 in metabolism. With this, the role of GPR54 in adipose tissue and in mediating obese conditions is clearly defined.

Knowing this, GPR54 is clearly well positioned to respond to secretions from adipocytes, considering its expression in adipose tissue. In this study, treatment of GPR-54 expressing cells with adipocyte-conditioned media did not significantly increase GPR54 activation relative to Opti-MEM, indicating that the adipocyte-conditioned media does not contain kisspeptin or any other endogenous ligand to GPR54. However, treatment with healthy adipocyte-conditioned medium resulted in significantly lower RLU/A420 compared to insulin-resistant treatment. These results pose two possibilities 1) an inverse agonist to GPR54 is present in only the healthy media and is decreasing the activation below basal activity or 2) there is a less potent agonist only present in the insulin-resistant adipocyte-conditioned medium increasing the RLU/A420 of GPR54-expressing cells. Wherein GPR54 knockout is associated with lower body weight and higher levels of energy metabolism, it stands to reason that GPR54 activation and expression would be higher in the insulin-resistant conditions (Tolson *et al.*, 2020). GPR54 was not screened directly against TNF- α in this study, and this should be completed to discover whether this cytokine is playing a role in mediating the difference in activation between the healthy and insulin-resistant conditions.

4.5.4 GPR142

GPR142 is an aromatic amino acid-sensing receptor, and its identified endogenous ligands are tryptophan and phenylalanine derivatives (Ueda *et al.*, 2018). Agonists of GPR142 have been identified as insulin secretagogues, classifying the key role of GPR142 in mediating insulin-resistance and type II diabetes (Wang *et al.*, 2016). In this study, RLU/A420 of GPR142-expressing cells was significantly downregulated relative to Opti-MEM in response to treatment with insulin-resistant adipocyte conditioned medium, but not healthy adipocyte conditioned medium, where it was not significantly changed from its basal

activity. This indicates that an inverse agonist to GPR142 could be secreted from the insulin-resistant adipocytes and is resulting in this decrease in activation. At this time, no inverse agonists of GPR142 have been proposed, though there have been preliminary studies categorizing a potent small molecule antagonist (Murakoshi *et al.*, 2017). With this, it is also possible that an antagonist is present in both media. If the adipose tissue are secreting tryptophan and phenylalanine derivatives, this secreted antagonist would inhibit them from activating the receptor, resulting in these lower RLU/A420 values. Due to the role of GPR142 in mediating insulin production and its expression pattern in the liver, it would be well positioned to respond through paracrine or endocrine mechanisms to small molecules secreted by these insulin-resistant adipocytes (Wang *et al.*, 2016).

4.5.5 GPR153

Another elusive class A orphan, GPR153 has no proposed endogenous ligands to date. GPR153 is highly expressed in central regions of the brain, and sequence homology has revealed that it shares the most similarity (20% sequence identity) with serotonin receptors (Sreedharan *et al.*, 2011). A potential role for GPR153 in modulating food intake has also been suggested, which could be helpful information for identifying its cognate ligands (Sreedharan *et al.*, 2011). In this study, the results surrounding GPR153 were very intriguing. This receptor had significantly increased RLU/A420 relative to Opti-MEM after treatment with healthy, but not insulin-resistant adipocyte-conditioned medium, though expression was still increased after insulin-resistant treatment. However, treatment with 2.5nm TNF- α , known to also be present in the insulin-resistant medium, significantly increased RLU/A420 of GPR153-expressing cells relative to Opti-MEM (Fig. 11). There are a few probable explanations to these results. It is likely that a GPR153 agonist is present in the healthy adipocyte conditioned medium and resulting in this increase in relative luminescence, and that this same agonist is not present in the insulin-resistant medium. Further, it is possible that the impact of TNF- α was lessened in the insulin-resistant adipocyte-conditioned medium by other molecules, rendering the response non-significant. With this, our results suggest that a molecule secreted by healthy adipocytes is a potential endogenous ligand for GPR153, and that TNF- α is as well. The relationship between GPR153 and TNF- α was further investigated by a dose response curve, however high variability made these results inconclusive

(Appendix 3). Another trial of dose response curve should be completed to properly express this relationship.

4.5.6 MAS1

Finally, MAS1 is a promiscuous class A orphan receptor. While as early as 2007 studies demonstrated the ability of MAS1 to mediate the activity of angiotensin (1-7) (ang (1-7)), several follow up studies failed to recreate the incidences of MAS1 activation and signaling in response to ang (1-7), and there was a lack of evidence for direct binding of ang (1-7) to MAS1 (Karnik *et al.*, 2017). However, the ang (1-7)-MAS1 axis remains the most studied pairing for MAS1 and ang (1-7) is the most promising proposed endogenous ligand for MAS1 (Karnik *et al.*, 2017). Ang (1-7) signaling is a vital component of the renin-angiotensin system, exerting a cardioprotective effect against Angiotensin II by inducing vasodilation and preserving endothelial function (Hoffmann *et al.*, 2017)

The significant increase in RLU/A420 of MAS1-expressing cells after treatment with healthy adipocyte-conditioned medium indicates that an MAS1 agonist is present in the healthy adipocyte-conditioned medium. The knowledge that angiotensin peptides, including ang (1-7) are secretory products of adipocytes, and that a local renin-angiotensin system (RAS) is present in adipose tissues provides support for this hypothesis and an explanation for this result (Cassis *et al.*, 2008). However, the more intriguing result is that treatment with insulin-resistant adipocyte-conditioned media did not result in a significant increase in RLU/A420 of MAS1-expressing cells. This indicates that either ang (1-7) is not expressed in the insulin-resistant adipocyte conditioned-medium, or that an antagonist to MAS1 is present and inhibiting its activation by ang (1-7). Ang (1-7) is produced from the conversion of Angiotensin II via the enzyme ACE2 (Cassis *et al.*, 2008). Some studies suggest that in diabetic tissues, under insulin-resistant conditions, ACE2 expression, and thus the degradation of Angiotensin II and production of Ang (1-7) is decreased (Reich *et al.*, 2008). This supports the lack of activation of MAS1 in insulin-resistant adipocyte-conditioned medium, where its agonist is either expressed at lower levels, or not at all. Analyses of the components of the media, as well as investigating what potential role TNF- α may have in the activation of this receptor, will be necessary to further support these claims.

4.6 Conclusions and further directions

This study showed that both healthy and insulin-resistant adipocyte conditioned media can modulate the activity of orphan GPCRs, and that six receptors appear to modulate the difference between healthy and insulin-resistant adipocyte-conditioned media. As previously mentioned, validation studies should be completed to categorize the activation of the 12 recommended receptors in response to adipocyte-conditioned media. Further, where TNF- α demonstrated the ability to modulate the activity of three receptors, the remainder of the receptors not included in the first study should be screened against TNF- α to expose the potential impact of this cytokine on receptor activation.

It was clearly demonstrated that adipocyte-conditioned media were altering receptor activation, and when possible, suggestions of potential agonists and antagonists have been proposed. However, adipocytes secrete a wide variety of bioactive molecules and thus the components of the media are unknown. Proteomic and metabolomic analyses of the adipocyte-conditioned media would allow for the identification of these signaling molecules, and then protein-protein separation techniques could be used to isolate these signaling molecules. Once isolated, future experiments could be conducted to categorize receptor activation and identify their potential endogenous ligands.

The knowledge gained by this study builds a basis of understanding of the potential connections between adipocytes and orphan GPCRs and provides a strong starting point for further investigation and potential deorphanization. This study elucidated that receptors vary greatly in their responses to external signaling molecules, specifically providing evidence that receptors can modulate the difference between healthy and insulin-resistant adipocytes. In all, this study has strong applicable findings to endogenous ligand classification and the potential of several orphan receptors in modulating disease. Further validation studies will hopefully allow for the application of these findings to the development of therapeutic treatments for type II diabetes, the long-term impact of this study.

5. References

- Alexander, S.P.H., Battey, J., Benson, H.E., Benya, R.V., Bonner, T.I., Davenport, A.P., Dhanachandra Singh, K., Eguchi, S., Harmar, A., Holliday, N., Jensen, R.T., Karnik, S., Kostenis, E., Liew, W.C., Monaghan, A.E., Mpamhanga, C., Neubig, R., Pawson, A.J., Pin, J.-P., Sharman, J.L., Spedding, M., Spindel, E., Stoddart, L., Storjohann, L., Thomas, W.G., Tirupula, K., Vanderheyden, P., 2020. Class A Orphans (version 2020.5) in the IUPHAR/BPS Guide to Pharmacology Database. IUPHAR/BPS Guide Pharmacol. CITE 2020. <https://doi.org/10.2218/gtopdb/F16/2020.5>
- Alexandraki, K., Piperi, C., Kalofoutis, C., Singh, J., Alaveras, A., Kalofoutis, A., 2006. Inflammatory process in type 2 diabetes: The role of cytokines. *Ann. N. Y. Acad. Sci.* 1084, 89–117. <https://doi.org/10.1196/annals.1372.039>
- Antolin-Fontes, B., Li, K., Ables, J.L., Riad, M.H., Görlich, A., Williams, M., Wang, C., Lipford, S.M., Dao, M., Liu, J., Molina, H., Heintz, N., Kenny, P.J., Ibañez-Tallon, I., 2020. The habenular G-protein-coupled receptor 151 regulates synaptic plasticity and nicotine intake. *Proc. Natl. Acad. Sci.* 117, 5502–5509. <https://doi.org/10.1073/pnas.1916132117>
- Barnea, G., Strapps, W., Herrada, G., Berman, Y., Ong, J., Kloss, B., Axel, R., Lee, K.J., 2008. The genetic design of signaling cascades to record receptor activation. *Proc. Natl. Acad. Sci.* 105, 64–69. <https://doi.org/10.1073/pnas.0710487105>
- Bassilana, F., Nash, M., Ludwig, M.-G., 2019. Adhesion G protein-coupled receptors: opportunities for drug discovery. *Nat. Rev. Drug Discov.* 18, 869–884. <https://doi.org/10.1038/s41573-019-0039-y>
- Black, J.B., Premont, R.T., Daaka, Y., 2016. Feedback regulation of G protein-coupled receptor signaling by GRKs and arrestins. *Semin. Cell Dev. Biol.* 50, 95–104. <https://doi.org/10.1016/j.semcdb.2015.12.015>
- Blüher, M., 2019. Obesity: global epidemiology and pathogenesis. *Nat. Rev. Endocrinol.* 15, 288–298. <https://doi.org/10.1038/s41574-019-0176-8>
- Boden, G., 2003. Effects of free fatty acids (FFA) on glucose metabolism: significance for insulin resistance and type 2 diabetes. *Exp. Clin. Endocrinol. Diabetes Off. J. Ger. Soc. Endocrinol. Ger. Diabetes Assoc.* 111, 121–124. <https://doi.org/10.1055/s-2003-39781>
- Brogi, S., Tafi, A., Désaubry, L., Nebigil, C.G., 2014. Discovery of GPCR ligands for probing signal transduction pathways. *Front. Pharmacol.* 5. <https://doi.org/10.3389/fphar.2014.00255>
- Buechler, C., Feder, S., Haberl, E.M., Aslanidis, C., 2019. Chemerin Isoforms and Activity in Obesity. *Int. J. Mol. Sci.* 20. <https://doi.org/10.3390/ijms20051128>

- Cassis, L.A., Police, S.B., Yiannikouris, F., Thatcher, S.E., 2008. Local Adipose Tissue Renin-Angiotensin System. *Curr. Hypertens. Rep.* 10, 93–98.
- Christian, S.L., Berry, M.D., 2018. Trace Amine-Associated Receptors as Novel Therapeutic Targets for Immunomodulatory Disorders. *Front. Pharmacol.* 9. <https://doi.org/10.3389/fphar.2018.00680>
- Coelho, M., Oliveira, T., Fernandes, R., 2013. Biochemistry of adipose tissue: an endocrine organ. *Arch. Med. Sci. AMS* 9, 191–200. <https://doi.org/10.5114/aoms.2013.33181>
- Cui, J., Ding, Y., Chen, S., Zhu, X., Wu, Y., Zhang, M., Zhao, Y., Li, T.-R.R., Sun, L.V., Zhao, S., Zhuang, Y., Jia, W., Xue, L., Han, M., Xu, T., Wu, X., 2016. Disruption of Gpr45 causes reduced hypothalamic POMC expression and obesity. *J. Clin. Invest.* 126, 3192–3206. <https://doi.org/10.1172/JCI85676>
- Davenport, A.P., Alexander, S.P.H., Sharman, J.L., Pawson, A.J., Benson, H.E., Monaghan, A.E., Liew, W.C., Mpamhanga, C.P., Bonner, T.I., Neubig, R.R., Pin, J.P., Spedding, M., Harmar, A.J., 2013. International Union of Basic and Clinical Pharmacology. LXXXVIII. G Protein-Coupled Receptor List: Recommendations for New Pairings with Cognate Ligands. *Pharmacol. Rev.* 65, 967–986. <https://doi.org/10.1124/pr.112.007179>
- Davenport, A.P., Maguire, J.J., Mead, E.J., Pawson, A.J., 2020. Kisspeptin receptor (version 2020.4) in the IUPHAR/BPS Guide to Pharmacology Database. *IUPHARBPS Guide Pharmacol. CITE 2020*. <https://doi.org/10.2218/gtopdb/F34/2020.4>
- D'Souza, K., Paramel, G.V., Kienesberger, P.C., 2018. Lysophosphatidic Acid Signaling in Obesity and Insulin Resistance. *Nutrients* 10. <https://doi.org/10.3390/nu10040399>
- Feng, X., Wang, W., Liu, J., Liu, Y., 2011. β -Arrestins: multifunctional signaling adaptors in type 2 diabetes. *Mol. Biol. Rep.* 38, 2517–2528. <https://doi.org/10.1007/s11033-010-0389-3>
- Fukushima, N., Chun, J., 2001. The LPA receptors. *Prostaglandins Other Lipid Mediat.* 64, 21–32. [https://doi.org/10.1016/s0090-6980\(01\)00105-8](https://doi.org/10.1016/s0090-6980(01)00105-8)
- Fuster, J.J., Ouchi, N., Gokce, N., Walsh, K., 2016. Obesity-induced Changes in Adipose Tissue Microenvironment and Their Impact on Cardiovascular Disease. *Circ. Res.* 118, 1786–1807. <https://doi.org/10.1161/CIRCRESAHA.115.306885>
- Gesta, S., Simon, M.-F., Rey, A., Sibrac, D., Girard, A., Lafontan, M., Valet, P., Saulnier-Blache, J.S., 2002. Secretion of a lysophospholipase D activity by adipocytes: involvement in lysophosphatidic acid synthesis. *J. Lipid Res.* 43, 904–910. [https://doi.org/10.1016/S0022-2275\(20\)30464-8](https://doi.org/10.1016/S0022-2275(20)30464-8)
- Green, H., Meuth, M., 1974. An established pre-adipose cell line and its differentiation in culture. *Cell* 3, 127–133. [https://doi.org/10.1016/0092-8674\(74\)90116-0](https://doi.org/10.1016/0092-8674(74)90116-0)

- Gurevich, V.V., Gurevich, E.V., 2019. The structural basis of the arrestin binding to GPCRs. *Mol. Cell. Endocrinol.* 484, 34–41. <https://doi.org/10.1016/j.mce.2019.01.019>
- Hardy, O.T., Czech, M.P., Corvera, S., 2012. What causes the insulin resistance underlying obesity? *Curr. Opin. Endocrinol. Diabetes Obes.* 19, 81–87. <https://doi.org/10.1097/MED.0b013e3283514e13>
- Heldin, C.-H., Lu, B., Evans, R., Gutkind, J.S., 2016. Signals and Receptors. *Cold Spring Harb. Perspect. Biol.* 8. <https://doi.org/10.1101/cshperspect.a005900>
- Hennen, S., Wang, H., Peters, L., Merten, N., Simon, K., Spinrath, A., Blättermann, S., Akkari, R., Schrage, R., Schröder, R., Schulz, D., Vermeiren, C., Zimmermann, K., Kehraus, S., Drewke, C., Pfeifer, A., König, G.M., Mohr, K., Gillard, M., Müller, C.E., Lu, Q.R., Gomeza, J., Kostenis, E., 2013. Decoding signaling and function of the orphan G protein-coupled receptor GPR17 with a small-molecule agonist. *Sci. Signal.* 6, ra93. <https://doi.org/10.1126/scisignal.2004350>
- Hoffmann Brian R., Stodola Timothy J., Wagner Jordan R., Didier Daniela N., Exner Eric C., Lombard Julian H., Greene Andrew S., 2017. Mechanisms of Mas1 Receptor-Mediated Signaling in the Vascular Endothelium. *Arterioscler. Thromb. Vasc. Biol.* 37, 433–445. <https://doi.org/10.1161/ATVBAHA.116.307787>
- Holmes, F.E., Kerr, N., Chen, Y.-J., Vanderplank, P., McArdle, C.A., Wynick, D., 2017. Targeted disruption of the orphan receptor Gpr151 does not alter pain-related behaviour despite a strong induction in dorsal root ganglion expression in a model of neuropathic pain. *Mol. Cell. Neurosci.* 78, 35–40. <https://doi.org/10.1016/j.mcn.2016.11.010>
- Hotamisligil, G.S., Peraldi, P., Budavari, A., Ellis, R., White, M.F., Spiegelman, B.M., 1996. IRS-1-mediated inhibition of insulin receptor tyrosine kinase activity in TNF-alpha- and obesity-induced insulin resistance. *Science* 271, 665–668. <https://doi.org/10.1126/science.271.5249.665>
- Hurt, R.T., Kulisek, C., Buchanan, L.A., McClave, S.A., 2010. The Obesity Epidemic: Challenges, Health Initiatives, and Implications for Gastroenterologists. *Gastroenterol. Hepatol.* 6, 780–792.
- Ijuin, T., Takenawa, T., 2012. Regulation of Insulin Signaling by the Phosphatidylinositol 3,4,5-Triphosphate Phosphatase SKIP through the Scaffolding Function of Pak1. *Mol. Cell. Biol.* 32, 3570–3584. <https://doi.org/10.1128/MCB.00636-12>
- Janssens, R., Struyf, S., Proost, P., 2018. The unique structural and functional features of CXCL12. *Cell. Mol. Immunol.* 15, 299–311. <https://doi.org/10.1038/cmi.2017.107>
- Jensen, A.A., Spalding, T.A., 2004. Allosteric modulation of G-protein coupled receptors. *Eur. J. Pharm. Sci. Off. J. Eur. Fed. Pharm. Sci.* 21, 407–420. <https://doi.org/10.1016/j.ejps.2003.11.007>

- Kahn, B.B., Flier, J.S., 2000. Obesity and insulin resistance. *J. Clin. Invest.* 106, 473–481. <https://doi.org/10.1172/JCI10842>
- Karnik, S.S., Singh, K.D., Tirupula, K., Unal, H., 2017. Significance of angiotensin 1–7 coupling with MAS1 receptor and other GPCRs to the renin-angiotensin system: IUPHAR Review 22. *Br. J. Pharmacol.* 174, 737–753. <https://doi.org/10.1111/bph.13742>
- Khan, M.Z., He, L., 2017. Neuro-psychopharmacological perspective of Orphan receptors of Rhodopsin (class A) family of G protein-coupled receptors. *Psychopharmacology (Berl.)* 234, 1181–1207. <https://doi.org/10.1007/s00213-017-4586-9>
- Kim, K.-M., Caron, M.G., 2008. Complementary roles of the DRY motif and C-terminus tail of GPCRS for G protein coupling and beta-arrestin interaction. *Biochem. Biophys. Res. Commun.* 366, 42–47. <https://doi.org/10.1016/j.bbrc.2007.11.055>
- Kimple, A.J., Bosch, D.E., Giguère, P.M., Siderovski, D.P., 2011. Regulators of G-protein signaling and their G α substrates: promises and challenges in their use as drug discovery targets. *Pharmacol. Rev.* 63, 728–749. <https://doi.org/10.1124/pr.110.003038>
- Kos, K., Harte, A.L., James, S., Snead, D.R., O'Hare, J.P., McTernan, P.G., Kumar, S., 2007. Secretion of neuropeptide Y in human adipose tissue and its role in maintenance of adipose tissue mass. *Am. J. Physiol.-Endocrinol. Metab.* 293, E1335–E1340. <https://doi.org/10.1152/ajpendo.00333.2007>
- Kroeze, W.K., Sassano, M.F., Huang, X.-P., Lansu, K., McCorvy, J.D., Giguère, P.M., Sciaky, N., Roth, B.L., 2015. PRESTO-Tango as an open-source resource for interrogation of the druggable human GPCRome. *Nat. Struct. Mol. Biol.* 22, 362–369. <https://doi.org/10.1038/nsmb.3014>
- Kwon, H., Pessin, J.E., 2013. Adipokines mediate inflammation and insulin resistance. *Front. Endocrinol.* 4, 71. <https://doi.org/10.3389/fendo.2013.00071>
- Lo, K.A., Labadorf, A., Kennedy, N.J., Han, M.S., Yap, Y.S., Matthews, B., Xin, X., Sun, L., Davis, R.J., Lodish, H.F., Fraenkel, E., 2013. Analysis of In Vitro Insulin-Resistance Models and Their Physiological Relevance to In Vivo Diet-Induced Adipose Insulin Resistance. *Cell Rep.* 5, 259–270. <https://doi.org/10.1016/j.celrep.2013.08.039>
- Luttrell, L.M., Lefkowitz, R.J., 2002. The role of β -arrestins in the termination and transduction of G-protein-coupled receptor signals. *J. Cell Sci.* 115, 455–465.
- Martin, A.L., Steurer, M.A., Aronstam, R.S., 2015. Constitutive Activity among Orphan Class-A G Protein Coupled Receptors. *PLOS ONE* 10, e0138463. <https://doi.org/10.1371/journal.pone.0138463>

- Mollica Poeta, V., Massara, M., Capucetti, A., Bonecchi, R., 2019. Chemokines and Chemokine Receptors: New Targets for Cancer Immunotherapy. *Front. Immunol.* 10, 379. <https://doi.org/10.3389/fimmu.2019.00379>
- Mueckler, M., 2001. Insulin resistance and the disruption of Glut4 trafficking in skeletal muscle. *J. Clin. Invest.* 107, 1211–1213.
- Murakoshi, M., Kuwabara, H., Nagasaki, M., Xiong, Y.M., Reagan, J.D., Maeda, H., Nara, F., 2017. Discovery and pharmacological effects of a novel GPR142 antagonist. *J. Recept. Signal Transduct. Res.* 37, 290–296. <https://doi.org/10.1080/10799893.2016.1247861>
- Murtazina, R.Z., Zhukov, I.S., Korenkova, O.M., Popova, E.A., Kuvarzin, S.R., Efimova, E.V., Kubarskaya, L.G., Batotsyrenova, E.G., Zolotoverkhaya, E.A., Vaganova, A.N., Apyratin, S.A., Alenina, N.V., Gainetdinov, R.R., 2021. Genetic Deletion of Trace-Amine Associated Receptor 9 (TAAR9) in Rats Leads to Decreased Blood Cholesterol Levels. *Int. J. Mol. Sci.* 22. <https://doi.org/10.3390/ijms22062942>
- Oishi, A., Karamitri, A., Gerbier, R., Lahuna, O., Ahmad, R., Jockers, R., 2017. Orphan GPR61, GPR62 and GPR135 receptors and the melatonin MT 2 receptor reciprocally modulate their signaling functions. *Sci. Rep.* 7, 8990. <https://doi.org/10.1038/s41598-017-08996-7>
- Oldham, W.M., Hamm, H.E., 2008. Heterotrimeric G protein activation by G-protein-coupled receptors. *Nat. Rev. Mol. Cell Biol.* 9, 60–71. <https://doi.org/10.1038/nrm2299>
- Rabe, K., Lehrke, M., Parhofer, K.G., Broedl, U.C., 2008. Adipokines and Insulin Resistance. *Mol. Med.* 14, 741–751. <https://doi.org/10.2119/2008-00058.Rabe>
- Reich, H.N., Oudit, G.Y., Penninger, J.M., Scholey, J.W., Herzenberg, A.M., 2008. Decreased glomerular and tubular expression of ACE2 in patients with type 2 diabetes and kidney disease. *Kidney Int.* 74, 1610–1616. <https://doi.org/10.1038/ki.2008.497>
- Rosenbaum, D.M., Rasmussen, S.G.F., Kobilka, B.K., 2009. The structure and function of G-protein-coupled receptors. *Nature* 459, 356–363. <https://doi.org/10.1038/nature08144>
- Rourke, J.L., Dranse, H.J., Sinal, C.J., 2015. CMKLR1 and GPR1 mediate chemerin signaling through the RhoA/ROCK pathway. *Mol. Cell. Endocrinol.* 417, 36–51. <https://doi.org/10.1016/j.mce.2015.09.002>
- Rourke, J.L., Muruganandan, S., Dranse, H.J., McMullen, N.M., Sinal, C.J., 2014. Gpr1 is an active chemerin receptor influencing glucose homeostasis in obese mice. *J. Endocrinol.* 222, 201–215. <https://doi.org/10.1530/JOE-14-0069>
- Ruisanchez, É., Dancs, P., Kerék, M., Németh, T., Faragó, B., Balogh, A., Patil, R., Jennings, B.L., Liliom, K., Malik, K.U., Smrcka, A.V., Tigyi, G., Benyó, Z., 2014.

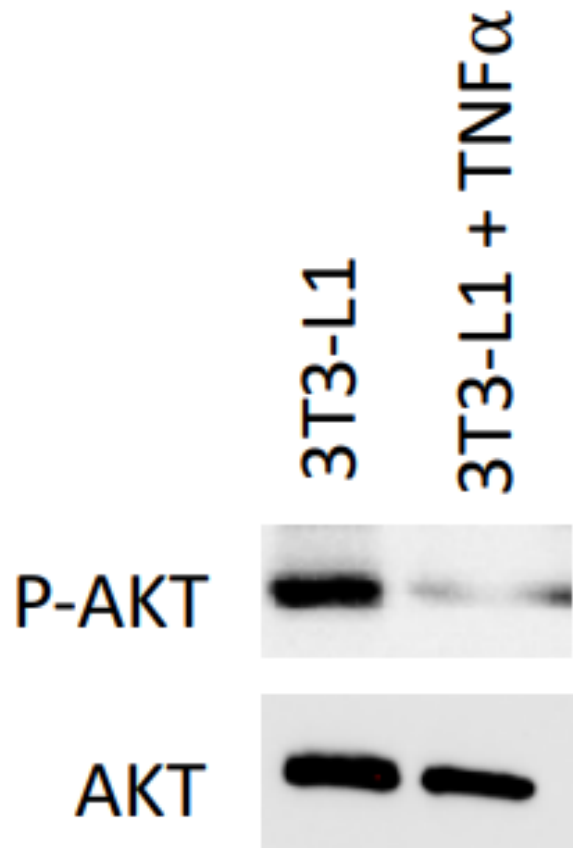
Lysophosphatidic acid induces vasodilation mediated by LPA1 receptors, phospholipase C, and endothelial nitric oxide synthase. *FASEB J. Off. Publ. Fed. Am. Soc. Exp. Biol.* 28, 880–890. <https://doi.org/10.1096/fj.13-234997>

- Shin, J., Fukuhara, A., Onodera, T., Kita, S., Yokoyama, C., Otsuki, M., Shimomura, I., 2018. SDF-1 Is an Autocrine Insulin-Desensitizing Factor in Adipocytes. *Diabetes* 67, 1068–1078. <https://doi.org/10.2337/db17-0706>
- Sikaris, K.A., 2004. The clinical biochemistry of obesity. *Clin. Biochem. Rev.* 25, 165–181.
- Spehr, M., Munger, S.D., 2009. Olfactory receptors: G protein-coupled receptors and beyond. *J. Neurochem.* 109, 1570–1583. <https://doi.org/10.1111/j.1471-4159.2009.06085.x>
- Sreedharan, S., Almén, M.S., Carlini, V.P., Haitina, T., Stephansson, O., Sommer, W.H., Heilig, M., Barioglio, S.R. de, Fredriksson, R., Schiöth, H.B., 2011. The G protein coupled receptor Gpr153 shares common evolutionary origin with Gpr162 and is highly expressed in central regions including the thalamus, cerebellum and the arcuate nucleus. *FEBS J.* 278, 4881–4894. <https://doi.org/10.1111/j.1742-4658.2011.08388.x>
- Sriram, K., Insel, P.A., 2018. G Protein-Coupled Receptors as Targets for Approved Drugs: How Many Targets and How Many Drugs? *Mol. Pharmacol.* 93, 251–258. <https://doi.org/10.1124/mol.117.111062>
- Suchý, T., Zieschang, C., Popkova, Y., Kaczmarek, I., Weiner, J., Liebing, A.-D., Çakir, M.V., Landgraf, K., Gericke, M., Pospisilik, J.A., Körner, A., Heiker, J.T., Dannenberger, D., Schiller, J., Schöneberg, T., Liebscher, I., Thor, D., 2020. The repertoire of Adhesion G protein-coupled receptors in adipocytes and their functional relevance. *Int. J. Obes.* 44, 2124–2136. <https://doi.org/10.1038/s41366-020-0570-2>
- Tabata, K., Baba, K., Shiraishi, A., Ito, M., Fujita, N., 2007. The orphan GPCR GPR87 was deorphanized and shown to be a lysophosphatidic acid receptor. *Biochem. Biophys. Res. Commun.* 363, 861–866. <https://doi.org/10.1016/j.bbrc.2007.09.063>
- Tolson, K.P., Marooki, N., De Bond, J.-A.P., Walenta, E., Stephens, S.B.Z., Liaw, R.B., Savur, R., Wolfe, A., Oh, D.Y., Smith, J.T., Kauffman, A.S., 2020. Conditional knockout of kisspeptin signaling in brown adipose tissue increases metabolic rate and body temperature and lowers body weight. *FASEB J. Off. Publ. Fed. Am. Soc. Exp. Biol.* 34, 107–121. <https://doi.org/10.1096/fj.201901600R>
- Ueda, Y., Iwakura, H., Bando, M., Doi, A., Ariyasu, H., Inaba, H., Morita, S., Akamizu, T., 2018. Differential role of GPR142 in tryptophan-mediated enhancement of insulin secretion in obese and lean mice. *PLoS ONE* 13. <https://doi.org/10.1371/journal.pone.0198762>
- Walther, C., Ferguson, S.S.G., 2013. Arrestins, in: *Progress in Molecular Biology and Translational Science*. Elsevier, pp. 93–113. <https://doi.org/10.1016/B978-0-12-394440-5.00004-8>

- Wang, J., Carrillo, J.J., Lin, H.V., 2016. GPR142 Agonists Stimulate Glucose-Dependent Insulin Secretion via Gq-Dependent Signaling. *PLoS ONE* 11. <https://doi.org/10.1371/journal.pone.0154452>
- Wang, T., Cui, X., Xie, L., Xing, R., You, P., Zhao, Y., Yang, Y., Xu, Y., Zeng, L., Chen, H., Liu, M., 2018. Kisspeptin Receptor GPR54 Promotes Adipocyte Differentiation and Fat Accumulation in Mice. *Front. Physiol.* 9. <https://doi.org/10.3389/fphys.2018.00209>
- Wang, Z., Zhou, W., Zheng, G., Yang, G., 2020. Inhibition of GPR17 with pranlukast protects against TNF- α -induced loss of type II collagen in ATDC5 cells. *Int. Immunopharmacol.* 88, 106870. <https://doi.org/10.1016/j.intimp.2020.106870>
- Zhang, Y., Scoumanne, A., Chen, X., 2010. G Protein-coupled receptor 87: A promising opportunity for cancer drug discovery. *Mol. Cell. Pharmacol.* 2, 111–116. <https://doi.org/10.4255/mcpharmacol.10.15>
- Zhao, H.-L., Liu, L.-Z., Sui, Y., Ho, S.K.S., Tam, S.-K., Lai, F.M.M., Chan, J.C.N., Tong, P.C.Y., 2010. Fatty acids inhibit insulin-mediated glucose transport associated with actin remodeling in rat L6 muscle cells. *Acta Diabetol.* 47, 331–339. <https://doi.org/10.1007/s00592-010-0225-1>

6. Appendix

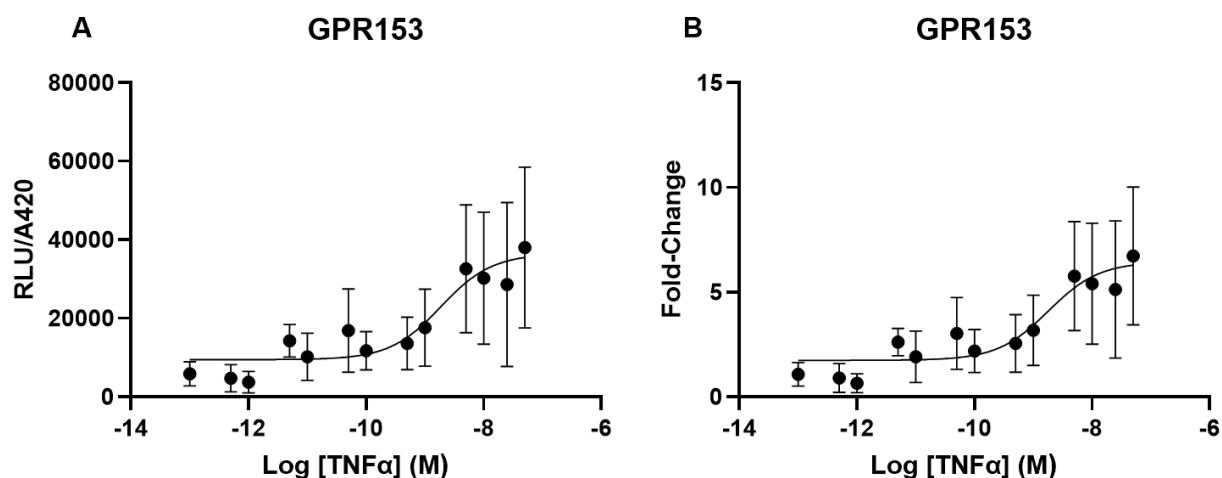
Appendix 1: TNF- α induces in vivo insulin resistance. Western blot analysis of phosphor-Akt protein expression from untreated (3T3-L1) and TNF- α treated (3T3-L1 + TNF α) 3T3-L1 adipocytes. Bottom panel shows quantification of protein level normalized to total Akt loading control. Data courtesy of N. McMullen.



Appendix 2: High Throughput Screen Results. The Fold-Change values relative to Opti-MEM of receptors from the HTS after treatment with healthy and insulin-resistant adipocyte-conditioned media. Data is presented as mean \pm SEM.

Receptor #	Receptor Name	Receptor Subfamily	Fold-Change Healthy	Fold-Change Insulin-Resistant
R2	GPER	Orphan Estrogen Receptor	1.26 \pm 0.14	1.62 \pm 0.291
R3	GPR101	Class A Orphan	0.604 \pm 0.101	0.73 \pm 0.109
R4	GPR110	Adhesion Class Orphan	1.07 \pm 0.145	1.47 \pm 0.213
R5	GPR113	Adhesion Class Orphan	1.21 \pm 0.366	0.830 \pm 0.207
R6	GPR116	Adhesion Class Orphan	0.506 \pm 0.090	0.505 \pm 0.0879
R7	GPR12	Class A Orphan	1.19 \pm 0.475	1.41 \pm 0.441
R8	GPR123	Adhesion Class Orphan	0.869 \pm 0.178	0.814 \pm 0.0787
R9	GPR132	Class A Orphan	1.08 \pm 0.197	1.91 \pm 0.389
R10	GPR133	Adhesion Class Orphan	0.474 \pm 0.076	0.408 \pm 0.104
R11	GPR141	Class A Orphan	0.582 \pm 0.124	0.584 \pm 0.0991
R12	GPR142	Class A Orphan	0.727 \pm 0.153	0.379 \pm 0.0538
R13	GPR143	Other 7TM orphan	0.762 \pm 0.207	0.663 \pm 0.0995
R14	GPR144	Adhesion Class Orphan	0.756 \pm 0.107	0.462 \pm 0.0915
R15	GPR146	Class A Orphan	3.00 \pm 1.01	2.77 \pm 0.970
R16	GPR148	Class A Orphan	1.71 \pm 0.479	1.48 \pm 0.285
R17	GPR149	Class A Orphan	1.90 \pm 0.326	1.64 \pm 0.428
R18	GPR15	Class A Orphan	2.85 \pm 0.513	2.89 \pm 0.628
R19	GPR150	Class A Orphan	2.15 \pm 0.489	3.58 \pm 1.14
R20	GPR151	Class A Orphan	3.18 \pm 0.664	4.48 \pm 1.43
R21	GPR153	Class A Orphan	6.71 \pm 1.08	4.49 \pm 1.80
R22	GPR156	Class C Orphan	3.35 \pm 1.58	5.35 \pm 0.650
R23	GPR160	Class A Orphan	1.99 \pm 0.343	2.37 \pm 0.497
R24	GPR161	Class A Orphan	2.68 \pm 0.773	2.82 \pm 1.06
R25	GPR162	Class A Orphan	1.21 \pm 0.123	1.05 \pm 0.0928
R26	GPR17	Class A Orphan	1.19 \pm 0.235	0.679 \pm 0.0508
R27	GPR171	Class A Orphan	0.436 \pm 0.094	0.386 \pm 0.0334
R28	GPR173	Class A Orphan	0.838 \pm 0.097	0.804 \pm 0.154
R29	GPR182	Class A Orphan	1.68 \pm 0.572	2.98 \pm 1.08
R30	GPR19	Class A Orphan	1.00 \pm 0.195	2.10 \pm 0.496
R31	GPR20	Class A Orphan	0.824 \pm 0.155	1.53 \pm 0.432
R32	GPR23	Orphan LPA Receptor	1.05 \pm 0.306	0.920 \pm 0.285
R33	GPR25	Class A Orphan	0.624 \pm 0.071	0.724 \pm 0.113
R34	GPR26	Class A Orphan	1.05 \pm 0.230	0.974 \pm 0.224
R35	GPR27	Class A Orphan	0.724 \pm 0.106	0.756 \pm 0.0960
R36	GPR31	Class A Orphan	0.762 \pm 0.112	0.912 \pm 0.178

R37	GPR32	Class A Orphan	0.190±0.025	0.244±0.0470
R38	GPR35	Class A Orphan	0.583±0.121	0.567±0.102
R39	GPR37	Class A Orphan	1.01±0.145	0.683±0.118
R40	GPR37L1	Class A Orphan	0.930±0.281	0.897±0.263
R41	GPR39	Class A Orphan	1.73±0.373	1.98±0.577
R42	GPR4	Class A Orphan	0.785±0.187	0.920±0.216
R43	GPR45	Class A Orphan	4.50±1.19	1.93±0.532
R44	GPR52	Class A Orphan	2.21±0.932	0.716±0.263
R45	GPR55	Class A Orphan	1.59±0.385	1.22±0.174
R46	GPR6	Class A Orphan	2.55±0.726	4.02±1.22
R47	GPR61	Class A Orphan	2.84±0.398	3.45±0.34
R48	GPR62	Class A Orphan	0.994±0.144	0.939±0.235
R49	GPR63	Class A Orphan	1.05±0.076	1.01±0.0432
R50	GPR64	Adhesion class orphan	3.00±0.527	2.29±0.416
R51	GPR78	Class A Orphan	4.06±0.659	3.89±0.597
R52	GPR83	Class A Orphan	2.15±0.258	1.53±0.212
R53	GPR84	Class A Orphan	1.63±0.251	1.97±0.259
R54	GPr85	Class A Orphan	1.93±0.595	1.51±0.366
R55	GPR87	Class A Orphan	2.62±0.700	2.68±0.691
R56	GPR88	Class A Orphan	2.70±0.460	3.25±0.271
R57	KISS (GPR54)	Orphan Kisspeptin Receptor	0.516±0.067	1.56±0.567
R58	MAS1	Class A Orphan	3.55±0.953	1.44±0.198
R59	MAS1L	Class A Orphan	1.75±0.152	2.22±0.352
R60	MRGPRD	Class A Orphan	1.91±0.506	1.77±0.231
R61	MRGPRF	Class A Orphan	0.961±0.237	1.14±0.170
R62	MRGPRG	Class A Orphan	1.70±0.380	1.92±0.326
R63	MRGPRX1	Class A Orphan	2.47±0.227	2.84±0.305
R64	MRGPRX2	Class A Orphan	1.71±0.268	2.78±0.647
R65	MRGPRX4	Class A Orphan	1.42±0.152	1.59±0.178
R66	OPN3	Orphan Opsin Receptor	1.17±0.073	1.09±0.131
R67	OPN5	Orphan Opsin Receptor	2.66±0.513	2.21±0.411
R68	PK2	Orphan Prokinectin Receptor	1.33±0.130	1.17±0.139
R69	PRP	Peptide Receptor	2.85±0.793	2.69±0.589
R70	TAAR5	Class A Orphan	3.51±0.750	3.21±0.862
R71	TAAR6	Class A Orphan	1.38±0.165	1.76±0.188
R72	TAAR9	Class A Orphan	2.15±0.162	1.65±0.113



Appendix 3: Dose-Dependent Activation of GPR153 in response to treatment with TNF α . Activation of GPR153 was quantified following a β -arrestin recruitment assay in which HTLA cells were transiently transfected with the receptor. A) The Relative Luminescence units (RLU) adjusted by β -galactosidase expression (A420; RLU/A420) of GPR153-transfected cells versus log₁₀ treatment concentration of TNF- α . B) The RLU/A420 Fold-Change data for A. Non-linear regression fit models were applied in Prism to A and B, from which an experimental EC₅₀ of 2.56E-09 M was calculated.